Phonons in nontransiton metals

E. G. Brovman and Yu. M. Kagan

I. V. Kurchatov Institute of Atomic Energy

Usp. Fiz. Nauk **112**, 369–426 (March 1974)

The article reviews the present status of the microscopic theory of non-transition-metal lattice vibrations. A regular scheme is described, which makes it possible to analyze in detail the role of the electrons in the formation of the phonon spectrum of metals. It is based on a consistent utilization of a small parameter V_K/ϵ_F, corresponding to the effective weakness of the interaction between the conduction electron and the ion core (V_K is the Fourier component of this interaction with a momentum transfer equal to one of the reciprocal-lattice vectors). Expansion of the electron-ion energy of the system in terms of this parameter yields, besides the pair interactions that are traditional for metals, also automatically the effective three-particle etc. unpaired inter-ion forces. It is shown that the unpaired forces play an important and sometimes decisive role in a number of questions, such as lattice stability, compressibility, the Cauchy relations for the elastic moduli, and singularities in the phonon spectrum. The theoretical analysis is illustrated by calculations of the static and dynamic properties of metals, and by comparison with experiment, using Na, Mg, Al, and β-Sn as examples.

CONTENTS

INTRODUCTION

Much progress was made recently in our knowledge of the dynamic properties of metals. The theory, which was phenomenological in character only recently, has become to a considerable degree a microscopic theory. It makes it possible to carry out an almost exhaustive qualitative and quantitative analysis for nontransition metals, making use of only elementary interactions that have clearcut physical nature.

This progress is connected primarily with the general development of the electron theory of metals, which occurred in the 60's. For the problem of formation of the phonon spectrum, an important role is played here precisely by the most highly developed and in fact initial ideas concerning the electron-ion system of nontransition metals (see, e.g., [1,2]). We can formulate them briefly as follows:

1. In metals, all the valence electrons are collectivized to form a single subsystem of quasifree electrons. The remaining ions have relatively small dimensions, occupying approximately 10% of the volume per atom in the crystal. Consequently, the ions in fact do not overlap and thus the direct interaction between the ions has a pure Coulomb character.

The allowance for the weak overlap or Van der Waals forces between the ions in such metals would almost certainly be less than the error of the theory at its contemporary state.

2. Strong oscillations of the wave function of the electron within the limits of the ionic core lead to a sharp decrease of the effective electron-ion interaction at short distances, and consequently also of the amplitude for the scattering of the electron by the ion at large momentum transfers. The success of the model of the quasifree electrons in the description of electrons near the Fermi surface is due precisely to the fact that in a regular metal an important role is played by electron scattering with transfer of a large momentum equal to the reciprocal-lattice vector.

3. Most frequently, the singularities of the wave function of the conduction electrons within the limits of the ionic core do not play a fundamental role in the analysis of the properties of a metal. This suggests the natural idea of replacing the true interaction with a multielectron ion by a certain effective single-particle potential (in the general case nonlocal), which is weaker than the initial potential inside the ion, but which retains the scattering properties of the initial ion. The resultant pseudopotential or model potential is usually determined from first principles or by using limited experimental information (see [1-3]).

Thus, if the ionic cores do not overlap the metal is a degenerate plasma with an electron density determined by the valence, and with a distinct effective electron-ion interaction vertex. This effective interaction is connected with a small parameter of the theory, namely the ratio V_K/ϵ_F, where V_K are the Fourier components of the effective potential at the points of the reciprocal lattice vector K (in the language of the local potential). It can be easily concluded from the foregoing that the phonons in the metal are low-frequency collective exci-

tations of the electron-ion plasma, the ground state of which corresponds to a regular arrangement of the ions. Therefore any consistent dynamic theory of metals should in principle be from the very outset a multiparticle theory, and should carry inevitably the imprint of the difficulties typical of multiparticle theory at intermediate densities (see, e.g., [4]).

At the same time, the theory of metals has developed so far principally by following the single-particle approach, and it is precisely in this way that it has attained the greatest quantitative success. The reason is that the dispersion properties of the electron spectrum on the Fermi surface, which can be described in principle in single-particle language, are most sensitive to the character of the electron-ion interaction, and it frequently suffices to take the electron-electron interaction into account in the form of a static screening of the potential of an isolated ion.

If, furthermore, the energy of the electron gas in a metal is obtained as the sum of single-particle energies calculated in second-order perturbation theory, then this energy contains a contribution that contains effectively the indirect pair interaction between ions via the conduction electrons [1,2]. When separated in explicit form, this interaction together with the direct Coulomb interaction constitutes the pair interaction between the ions, which can already be used to determine the vibrational spectrum within the framework of the traditional Born-Karman scheme [5,6]. An alternative analysis, in which the indirect interaction between two ions is determined directly with the screening taken self-consistently into account (see, e.g., the review [7]), or else the determination of the electron-gas energy in the Hartree-Fock approximation in second order in the electron-ion interaction, leads in fact to the same result. The only difference might lie in the different degree of accuracy in the allowance for the screening. Most of the work on the analysis of the phonon spectrum in particular metals was performed in this approximation (see the review [2] for the corresponding references). A particular place among these investigations is occupied by the research of Toya [8] and Vosco et al. [9]. Toya was the first to try and find the phonon spectrum of a metal by starting from a microscopic approach. Vosco et al. [9] made the first serious attempt to analyze the entire problem as a whole, and their paper still remains one of the best in this field (although somewhat different methods were used in the two references, in the final analysis the physical approximations turn out to be equivalent). Inasmuch as the approach remains in many respects single-particle, it follows, just as in the case of the electron spectrum, that the main emphasis of most studies was on the determination of the effective electron-ion interaction, a metal characteristic that is more readily atomic than pertaining to the solid state. Frequently, an illusion was created that this rather simplified approximation is valid, and the entire inaccuracy of the results was attributed only to the limited knowledge of the true value of the electron-ion interaction and of the dielectric function of the homogeneous electron gas.

The real picture of multiparticle interaction in a metal is actually much more complicated. Besides the pair interaction, there exists an unpaired interaction which is an indirect interaction via the conduction electrons of three or more ions. This interaction plays a fundamental role, particularly in the dynamics of vibrations (see below), and determines, in particular, the appearance of forces of the covalent type in a metal. A consistent examination of this interaction entails already significant formal difficulties, since it becomes necessary to take into account, simultaneously with the change in the electron spectrum, the influence of the restructuring of the electronic wave functions in the crystal on the character of the ion screening and on the Coulomb-interaction energy of the electron gas.

Recent papers [10,11] consider a certain general microscopic approach to the analysis of crystal dynamics, which expresses the force constants or the elements of the dynamic matrix in terms of the total reciprocal matrix of the dielectric constant, pertaining to all the electrons of the substance. (The first formulation of the dynamic problem in the language of the reciprocal dielectric matrix, in the Hartree approximation, was given for metals in a paper by Sham [12].) In this general form, the obtained representation is valid in principle for any substance, and can therefore be used to obtain limiting relations of general type. Unfortunately, it is very difficult to use it constructively for an analysis of the dynamics of a metal if an attempt is made to take multi-ion effects into account in a manageable approximation. As a result, the approximation used by Sham to calculate the phonons in Na [12] turns out again to be fully equivalent to the pair-interaction approximation. An attempt to take partial account of multi-ion interaction in a metal within the framework of this approach was actually made by Maradudin and Koppel [13,14].

The present authors have developed [15-17] a multiparticle theory of metals, in which it is possible to take consistently into account both paired and unpaired interion interaction via the conduction electrons. The analysis is based on the use, from the very outset, of a plasma Hamiltonian with introduction of an effective model potential in the vertex of the electron-ion interaction, and with determination of the ground-state energy as a functional of a static ion configuration. This energy is determined in the form of a series in powers of the electron-ion interaction, and the electron-electron interaction in each term of this series can be taken into account accurately. From the physical point of view, the obtained expansion describes in explicit form in succession two-ion, three-ion, etc. indirect interactions, and from the formal point of view it degenerates into a series in powers of a small parameter V_K/ϵ_F. Knowing the ground-state energy and assuming the validity of the adiabatic approximation, it is easy to determine the dynamic matrix of the oscillations, and also other metal characteristics integrated over the electron spectrum, such as the equation of state, compressibility, elastic modulus, etc.

This approach will be used here for the purpose of analyzing, in a unified manner, all the common problems of metal dynamics (the nature and role of covalence, the compressibility problem, singularities in the phonon spectrum, dynamic stability, etc.). On the other hand, the explicit determination of the phonon spectrum and of the principal characteristics of nontransition metals within the framework of this approach demonstrates that the present state of the theory makes it possible to describe many quantities, with reasonable quantitative accuracy, within the framework of a single set of approximations, using information only on the electron-ion interaction. It seems to us that this is precisely in general the main problem of the quantitative physical theory.

1. ADIABATIC APPROXIMATION IN A METAL

As is well known, the Born-Oppenheimer adiabatic approximation plays a cardinal role in the dynamic theory of lattices[5]. At first glance it seems that the main adiabaticity criterion, the absence of excitations with energy on the scale of the nuclear-vibration frequency ω from the electronic spectrum, is violated in a metal. Actually, it is possible to have near the Fermi surface electronic transitions with arbitrarily small excitation energy, and the adiabatic approximation does not hold at any rate for electrons in a layer on the order of ω. At the same time, however, for the bulk of the collectivized electrons, the excitation energy is of the order of ϵ_F, and by virtue of this they should follow adiabatically the vibrating nuclei. The latter circumstance makes it possible in fact to use the adiabatic approximation to determine quantities integrated over the electron spectrum. This problem is analyzed in detail in a paper by Chester[18] or in our paper[15]. In the latter paper, the principal attention is paid to the question of the renormalization of the adiabatic phonons as a result of the electron-phonon interaction at an arbitrary phonon momentum. Obviously, it is precisely this problem which is decisive for an estimate of the accuracy of the adiabatic approximation when determining the phonon spectrum of the metal. To solve the problem during the first stage, one can use the traditional procedure of separating the electronic and ionic degrees of freedom. If the Hamiltonian of the system is

$$\mathcal{H} = \mathcal{H}_e(\mathbf{r}) + \mathcal{H}_i(\mathbf{R}) + \mathcal{H}_{ei}(\mathbf{r}, \mathbf{R}), \tag{1.1}$$

then, separating the Schrödinger equation for the electrons at a fixed ion position,

$$[\mathcal{H}_e(\mathbf{r}) + \mathcal{H}_{ei}(\mathbf{r}, \mathbf{R})]\,\Psi_m(\mathbf{r}, \mathbf{R}) = E_m(\mathbf{R})\,\Psi_m(\mathbf{r}, \mathbf{R}), \tag{1.2}$$

we go over directly to a system of equations describing the vibrational problem:

$$[\mathcal{H}_i(\mathbf{R}) + E_n(\mathbf{R})]\,\Phi_n(\mathbf{R}) + \sum_m (A_{nm} + B_{nm})\,\Phi_m(\mathbf{R}) = E\Phi_n(\mathbf{R}), \tag{1.3}$$

where

$$A_{nm} = -\frac{1}{M}\sum_j (\nabla_{\mathbf{R}_j})_{nm}\nabla_{\mathbf{R}}, \quad B_{nm} = -\frac{1}{M}\sum_j (\nabla^2_{\mathbf{R}_j})_{nm} \tag{1.4}$$

($\mathbf{R}_j$ is the coordinate of the j-th ion, and the remaining notation is standard).

If we neglect the off-diagonal terms A_{nm} and B_{nm}, then (1.3) is an equation that determines the adiabatic vibrational spectrum, and the off-diagonal terms describe the non-adiabatic interaction of the vibrational and electronic systems.

The next step is the determination of the nonadiabatic part ΔE of the total energy. To this end we can change over to the second-quantization representation with respect to the electrons in the regular lattice and the adiabatic phonons, and use a relation that follows directly from (1.2):

$$(\nabla_{\mathbf{R}_j})_{nm} = -\frac{[\nabla_{\mathbf{R}_j}, \mathcal{H}_{ei}(\mathbf{r}, \mathbf{R})]_{nm}}{E_n(\mathbf{R}) - E_m(\mathbf{R})}. \tag{1.5}$$

If ΔE is obtained, then the renormalizations $\delta\omega_{q\lambda}$ of the phonons and δE_k of the electrons, due to the electron-phonon interaction, can be obtained by using the procedure of varying the energy of the system with respect to the corresponding occupation number, a procedure analogous to that used in the Landau theory of the Fermi liquid[19].

We then have

$$\delta\omega_{q\lambda} = \frac{\delta(\Delta E)}{\delta N_{q\lambda}}, \qquad \delta\varepsilon_{\mathbf{k}} = \frac{\delta(\Delta E)}{\delta n_{\mathbf{k}}} \tag{1.6}$$

($\mathbf{q}$ and λ are the wave number and the number of the phonon mode, and $\mathbf{k}$ is the wave vector of the electron).

Such a program was implemented (see[15]) and the energy ΔE was determined by perturbation theory in second order in A and in first order in B. Referring to the reader to that paper for details, we present only the final result for the renormalization of the phonons:

$$\delta\omega_{q\lambda} = \sum_{\mathbf{k}} |M_{\mathbf{k}q\lambda}|^2 \frac{n_{\mathbf{k}} - n_{\mathbf{k}+\mathbf{q}}}{E_{\mathbf{k}} - E_{\mathbf{k}+\mathbf{q}} - \omega_{q\lambda} + i\delta} - \sum_{\mathbf{k}} |M_{\mathbf{k}q\lambda}|^2 \frac{n_{\mathbf{k}} - n_{\mathbf{k}+\mathbf{q}}}{E_{\mathbf{k}} - E_{\mathbf{k}+\mathbf{q}}}, \tag{1.7}$$

where $M_{\mathbf{k},q\lambda}$ is the standard Bloch matrix element of the electron-phonon interaction and $n_{\mathbf{k}}$ are the occupation numbers for the electrons.

It is easy to understand the meaning of the presented expression. The second term in it describes the adiabatic contribution of the electrons to the frequency of the phonon excitation, and can itself be of order $\omega_{q\lambda}$. However, the nonadiabatic renormalization itself is quite weak. For the predominant part of phase space, (1.7) yields

$$\Delta\omega_{q\lambda} = \mathrm{Re}\,\delta\omega_{q\lambda} \sim \omega_{q\lambda}\left(\frac{\omega_0}{\varepsilon_F}\right)^2. \tag{1.8}$$

The damping $\Gamma_{q\lambda}$ is determined only by the first term of (1.7), by virtue of which it is not sensitive to the adiabatic procedure, and the estimate for $\Gamma_{q\lambda}$ is standard:

$$\Gamma_{q\lambda} = \mathrm{Im}\,\delta\omega_{q\lambda} \sim \omega_{q\lambda}\frac{\omega_0}{\varepsilon_F}. \tag{1.9}$$

In a narrow region of the momenta, where $|\mathbf{q} - 2\mathbf{k}_F|/k_F \sim \omega_0/\epsilon_F$, a larger shift in comparison with (1.8) takes place:

$$\Delta\omega_{q\lambda} \sim \omega_{q\lambda}\frac{\omega_0}{\varepsilon_F}. \tag{1.8'}$$

For the renormalization of the electron spectrum, the variational procedure (1.6) leads to the expression (we retain only the principal term)

$$\Delta\varepsilon_{\mathbf{k}} = \sum_{q,\lambda} |M_{\mathbf{k}q\lambda}|^2 \frac{\omega_{q\lambda}(1 - 2n_{\mathbf{k}+\mathbf{q}})}{(\varepsilon_{\mathbf{k}} - \varepsilon_{\mathbf{k}+\mathbf{q}})^2 - \omega^2_{q\lambda}}. \tag{1.10}$$

A simple analysis shows that far from the Fermi surface

$$\Delta\varepsilon_{\mathbf{k}} \sim \omega_0\frac{\omega_0}{\varepsilon_F},$$

whereas in a narrow "crust" $|\epsilon_{\mathbf{k}} - \epsilon_F| \sim \omega_0$ the renormalization of the electron velocity turns out to be already significant and does not contain the parameter ω_0/ϵ_F. The last result was first obtained by Migdal[20].

The foregoing estimates enable us to formulate general conclusions concerning the use of the adiabatic approximation in a metal and the role of electron-phonon interaction:

1) The phonon mode of the excitations in a metal can be separated with high accuracy within the framework of the pure adiabatic approximation. Allowance for the influence of the electron-phonon interaction on the dispersion law leads to a very weak renormalization.

2) The microscopic quantities determined from the microscopic analysis within the framework of the adiabatic approximation are determined with accuracy not lower than ω_0/ϵ_F.

3) To determine the properties connected with the electrons of the metal on the Fermi surface, in zeroth order in the parameter ω_0/ϵ_F, it is necessary, after obtaining the adiabatic phonon spectrum and the electron spectrum in the static lattice, to renormalize the electrons near the Fermi surface to allow for the electron-phonon interaction.

4) The renormalization of the phonons, in the general case, does not impose on the electron-phonon interaction constant any limitations that follow from the requirement of lattice stability. The converse statement, which results from the use of the Fröhlich Hamiltonian (see, e.g., [21,22]) is incorrect and is connected with the fact that the electron-ion interaction, roughly speaking, is taken into account twice, once in the choice of the "bare" phonons, which have a normal longitudinal sound, and the second time in the calculation of the renormalization of the form of the first term in (1.7). We note that this result is quite important for the superconductivity problem.

The validity of the adiabatic approximation greatly facilitates the application of field-theoretical methods[23] to the analysis of the dynamics of a metal. It is clear from the foregoing that the problem of finding the phonon spectrum reduces in this case in fact to a determination of the energy of the interacting electron gas in a static field of fixed ions, for which a diagram technique can be used directly.

Within the framework of the field-theoretical methods, it is also possible to use another approach based on the determination of the renormalization of the "bare" phonons due to the electron-phonon interaction[20]. An important role is played then by the results obtained by Migdal, namely that the vertex part of the electron-phonon interaction reduces, accurate to the same adiabaticity parameter ω_0/ϵ_F, to a simple vertex. It is important, however, that the electron-ion system of a metal cannot be reduced in a self-consistent manner to a system of "bare" electrons and phonons with a definite interaction between them (the Fröhlich Hamiltonian), which would be the analog of the situation in quantum electrodynamics. The reason is that introduction of any "bare" phonons in a metal already presupposes automatically participation of electrons in their formation. Therefore, the use of the Fröhlich Hamiltonian is certainly model dependent. This model turns out to be adequate when it comes to the influence of electron-phonon interaction on the electrons near the Fermi surface, for example, for the description of the electron kinetics, to the renormalization of the mass and lifetime of the electrons[20], to obtain equations for the gap in superconductivity theory (see, e.g., [24,25]), etc.

We note from a purely procedural point of view that in these problems, when using adiabatic phonons, it is necessary to leave all the phonon lines unrenormalized. (In particular, the result obtained for the mass operator actually coincides here with (1.10).)

A complete analysis of the nonadiabatic interaction of the electrons and phonons is, however, beyond the scope of the present article and should be the subject of a special review.

We note also that it is possible, in field-theoretical language, to consider the problem consistently by choosing as the "bare" Bose excitations the plasma oscillations of the ions in an immobile neutralized electron background, and by taking into account simultaneously the electron-electron and the electron-phonon interaction with the vertex determined by the "bare" electron-ion potential. Such a problem was analyzed, for example, in Schrieffer's book[25], using the "jellium" model. A consistent analysis with allowance for the discrete structure of the metal should lead in principle to a phonon spectrum that coincides with the spectrum of the adiabatic phonons obtained within the framework of the results given above.

The analysis that follows is based on the first approach, i.e., on the determination of the energy of the interacting electrons as a function of the ion position. For the purpose of our review, this approach offers significant advantages, since it makes it possible to obtain in a unified manner both the properties of the static lattice of the metal and the phonons in the lattice, and at the same time is the most lucid from the point of view of an analysis of the physical nature of the interactions responsible for the formation of these quantities.

2. ELECTRON ENERGY

As follows from the preceding chapter, to determine the electronic contribution to the formation of the vibrational spectrum it is necessary to find the energy $E(\mathbf{R}_1, \ldots, \mathbf{R}_n)$ of the electron system in the field of fixed ions; in Eq. (1.3) for the adiabatic phonons this energy plays the role of the potential energy. It suffices here to consider the problem at T = 0, inasmuch as at a fixed unit volume the corrections to the energy for the finite temperature are proportional to $(T/\epsilon_F)^2$.

We are therefore dealing here with the determination of the ground-state energy for the Hamiltonian contained in (1.2). In the second-quantization representation with respect to plane waves we have

$$\hat{\mathcal{H}} = \sum_{\mathbf{k}} \varepsilon_{\mathbf{k}} a_{\mathbf{k}}^{+} a_{\mathbf{k}} + \frac{1}{2} \sum_{\mathbf{k}\mathbf{k}'\mathbf{q}} \frac{4\pi e^2}{\Omega q^2} a_{\mathbf{k}-\mathbf{q}}^{+} a_{\mathbf{k}'+\mathbf{q}}^{+} a_{\mathbf{k}'} a_{\mathbf{k}} + \sum_{\mathbf{k}\mathbf{q}} U_{\mathbf{k},\mathbf{k}+\mathbf{q}} a_{\mathbf{k}}^{+} a_{\mathbf{k}+\mathbf{q}} \quad \left(\varepsilon_{\mathbf{k}} = \frac{\mathbf{k}^2}{2m}\right); \tag{2.1}$$

here Ω is the total volume of the system. The interaction of the electron with the ion system is given here by

$$U_{\mathbf{k},\mathbf{k}+\mathbf{q}} = V_{\mathbf{k},\mathbf{k}+\mathbf{q}} \frac{1}{N} \sum_{m} \exp(i\mathbf{q}\mathbf{R}_m), \tag{2.2}$$

where N is the total number of ions. (We confine ourselves for simplicity to a monatomic metal.)

For the vertex $v_{\mathbf{k},\mathbf{k}+\mathbf{q}}$ of the interaction between the electron and the individual ion we use the concept of a "weak" pseudopotential that takes into account effectively the cancellation of the interaction within the ionic core, (see the introduction) and describes correctly the amplitude for the scattering of the electron by an isolated ion. In the general case this model potential is nonlocal, and when it can be reduced to a local potential, the matrix element depends only on the momentum difference

$$V_{\mathbf{k},\mathbf{k}+\mathbf{q}} \to V_{\mathbf{q}}. \tag{2.3}$$

To simplify matters, we obtain first the principal results just for a local pseudopotential, and then analyze specially the changes that must be taken into account when nonlocality is introduced (see Chap. 12).

The ground-state energy of the electron system will be sought in the form of an expansion in powers of the electron-ion interaction. It is easy to write down the general form of this expansion:

$$E_e = E^{(0)} + E^{(1)} + E^{(2)} + E^{(3)} + \ldots, \tag{2.4}$$

$$E^{(n)} = \Omega \sum_{q_1 \dots q_n} \Gamma^{(n)}(q_1 \dots q_n) U_{q_1} \dots U_{q_n} \Delta(q_1 + \dots + q_n); \quad (2.5)$$

$\Delta(\mathbf{q})$ describes here the momentum conservation law corresponding to homogeneity of space. The many-pole quantities $\Gamma^{(n)}$ introduced in this manner are universal characteristics. They depend, obviously, only on the electron-electron interaction and do not depend on the positions of the ions or on the properties of the particular ion. It follows from (2.5) that the $\Gamma^{(n)}$ can be regarded, without loss of generality, as symmetrized over all their arguments.

To find the explicit form of (2.4) and (2.5), we can use a diagram technique (see, e.g., [23]), taking the perturbation in the S matrix to be the operator

$$\mathscr{H}_{\text{int}} = \mathscr{H}_{ee} + \mathscr{H}_{ei},$$

where $\mathscr{H}_{ee}$ and $\mathscr{H}_{ei}$ are respectively the second and third terms in (2.1). The ground-state energy can in this case be set in correspondence with an aggregate of "coupled" vacuum diagrams. Each term in (2.4) corresponds to the aggregate of all diagrams of a definite order in $\mathscr{H}_{ei}$ and of arbitrary order in $\mathscr{H}_{ee}$.

By virtue of the adiabaticity of the problem, the electron-ion interaction plays in these diagrams the role of the static external field. To each term of definite order in $\mathscr{H}_{ei}$ there corresponds a diagram given in Fig. 1, with an appropriate number of external-field wavy lines.

It should be borne in mind that the coefficients preceding such a diagram are not equal to unity, as in the case of the Green's function where the number of convolutions that lead to a given diagram cancels out 1/n! of the order of the diagram. It is easily seen that for "coupled" diagrams of the considered type, containing an external field $\mathscr{H}_{ei}$, the coefficient will always depend on the number n of external field lines, and after symmetrization with respect to the external momenta it is equal exactly to 1/n, since a cyclic permutation does not change the convolutions contained in the integral, and a symmetrized set of diagrams obviously has a symmetry of this type. It is essential that the coefficient does not depend on the order of the diagram with respect to the electron-electron interaction, since the external field "clamps" the ends and therefore acts like an external operator when the Green's function is written out in accordance with Wick's theorem.

When any multiparticle problem is considered for a metal, it is convenient to take into account in the very initial Hamiltonian (1.1) the electro-neutrality condition in explicit form. In the Fourier representation (this can be done even before the second quantization) the electroneutrality leads to a vanishing of the components of the Coulomb interaction with q = 0 in all three terms of (1.1). These components should therefore be missing from the Hamiltonian (2.1), and the "bare" ion-ion interaction should therefore be considered henceforth together with the negative homogeneous compensating background. It must be recognized here, however, that since the ion is not pointlike, we always have at small q

$$V_{q \to 0} = -\frac{4\pi z e^2}{q^2 \Omega_0} + \frac{b}{\Omega_0}, \quad (2.6)$$

where z is the charge of the ion and Ω_0 is the volume per ion. Therefore, when all the Coulomb interactions cancel each other at q = 0, the electron-ion potential retains a non-Coulomb part averaged over the volume. Accordingly, we must leave in the Hamiltonian (2.1), at q = 0,

$$V_{q=0} = \frac{b}{\Omega_0}. \quad (2.7)$$

The resultant effect of homogeneous potential plays a very important role in the determination of the different properties of the metal (see below), and vanishes only in the case of metallic hydrogen (see [30]).

We proceed now to a regular analysis of the individual many-pole functions $\Gamma^{(n)}$. The function $\Gamma^{(1)}$ is described by the single diagram indicated in Fig. 2, where the thick line denotes the total Green's function G of the electron, and it is easily seen that all the possible complications introduced in the diagram by the electron-electron interaction are included in the Green's function.

Therefore (the notation is standard; see [23])

$$\Gamma^{(1)}(0) = -2i \int \frac{d^4p}{(2\pi)^4} G(p) = n_0, \quad (2.8)$$

where n_0 is the density of the electron gas. In accordance with (2.5) and (2.7), we obtain here

$$E^{(1)} = N b z / \Omega_0 \quad (2.9)$$

(we have taken the fact that $n_0 = z/\Omega_0$ into account). Together with the energy of the homogeneous electron gas $E^{(0)}$, this term forms the structureless part of the total energy, which plays the major role for the volume properties of the metal and does not play any role in the formation of the vibrational spectrum. For $\Gamma^{(2)}$ we have the graphic equation shown in Fig. 3, where the dashed line denotes the interelectron interaction line, and $\pi(\mathbf{q})$ denotes a block that is irreducible (non-intersectable) with respect to this line and represents in fact the static polarization operator. The summation is carried out directly. As a result we get

$$\Gamma^{(2)}(\mathbf{q}, -\mathbf{q}) = -\frac{1}{2} \frac{\pi(\mathbf{q})}{\varepsilon(\mathbf{q})}, \quad (2.10)$$

where

$$\varepsilon(\mathbf{q}) = 1 + \frac{4\pi e^2}{q^2} \pi(\mathbf{q}) \quad (2.11)$$

is the static dielectric constant of the homogeneous electron gas.

We consider now the function $\Gamma^{(n)}$ at an arbitrary value of n. What is important is that the diagrams of the described type (see Fig. 1) admits of partial summation corresponding to replacement of each external-field line by a "thick" line with the aid of the graphic relation shown in Fig. 4. This leads to the expression

$$\Gamma^{(n)}(q_1, \dots, q_n) = \frac{\Lambda^{(n)}(q_1, \dots, q_n)}{\varepsilon(q_1) \dots \varepsilon(q_n)} \quad (n > 2), \quad (2.12)$$

where $\Lambda^{(n)}$ is the aggregate of diagrams with n external-field lines containing no blocks (polarization parts) that might be attributed to "thick" external lines. Further

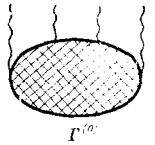

FIG. 1

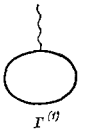

FIG. 2

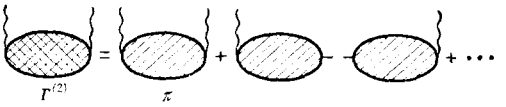

FIG. 3

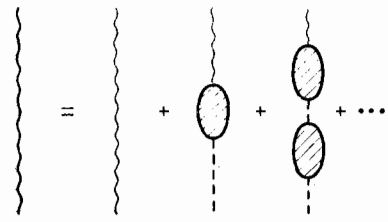

FIG. 4

simplication of $\Gamma^{(n)}$ depends already on the concrete approximation (see below).

The terms starting with n = 4 call for a special analysis, since the usual perturbation-theory technique for finding the ground state does not apply to them. More accurately speaking, the total energy determined with its aid will no longer correspond to a system state with the lowest energy. The reason is that starting with n = 4 it is necessary, when determining the ground state, to take into account from the very outset the distortion of the shape of the Fermi surface, whereas in perturbation theory we continue to follow the spherical filling in momentum space, which is characteristic of the ground state of the unperturbed system. In other words, a change peculiar to the crystal takes place in the symmetry of the ground state, and to take this change into account it is necessary to modify the standard perturbation theory in such a way as to ensure additional variation with respect to the shape of the Fermi surface. It is possible to use instead a thermodynamic perturbation theory[23], in which the lower energy states are automatically selected, and then let $T \to 0$.

The actual procedure consists of finding the thermodynamic potential Ω by summing diagrams having a perfectly analogous structure, but defined now for the temperature Green's functions, and then change over from Ω (as a function of the chemical potential μ) to the system energy E (as a function of the particle number N). The expansions for both Ω and E take the forms (2.4) and (2.5). It is natural also that the partial-summation procedure that has led to (2.12) remains in force for the coefficients of the series for Ω. On going to E, the resultant many-pole function $\Omega^{(n)}$ becomes generally speaking renormalized and equal to

$$\Lambda^{(n)}(q_1, \ldots, q_n) = \Lambda_\Omega^{(n)}(q_1, \ldots, q_n) + \Lambda_\mu^{(n)}(q_1, \ldots, q_n). \quad (2.13)$$

Here Λ_μ is the result of renormalization of the chemical potential, and differs from zero only at $n \geq 4$ and only for a rigorously defined set of momenta **q**. Thus, at n = 4 the only nonvanishing component is

$$\Lambda_\mu^{(4)}(q_1, -q_1, q_2, -q_2) = \frac{1}{24}\frac{\partial\mu}{\partial n_0}\left(\frac{\partial\pi(q_1)}{\partial\mu}\right)_0\left(\frac{\partial\pi(q_2)}{\partial\mu}\right)_0. \quad (2.14)$$

For the same set of external momenta (when the sum of several successive q_i vanishes, i.e., when the arguments of two or several G functions coincide), a unique "anomalous" contribution appears in the temperature technique for Ω, on going to the limit as $T \to 0$, besides the usual contribution corresponding to the diagram expansion of the energy (T = 0). We note that "anomalous" contributions appeared first in the problem of a Fermi gas with nonspherical interaction[29]. At arbitrary external momenta not corresponding to special conditions, both the "anomalous" contributions and the term Λ_μ are missing, and $\Lambda^{(n)}$ can be determined by the standard perturbation theory.

We can now find the structure-dependent part of the electron energy. We note to this end, taking (2.2) into account, that the n-th term of the series contains n ion coordinates, so that $E^{(2)}$ contains the coordinates of a pair of ions, i.e., corresponds to the effective pair interaction, while $E^{(n)}$ contains the coordinates of n ions and corresponds to pairwise indirect interaction between n ions via the conduction electrons.

The expressions obtained above are valid, naturally, for any fixed ion configuration. When determining the static part of the pair energy in an irregular system (for example, in liquid metal), it is necessary to average over the possible configurations, and in a regular crystal, owing to the interference, a very great simplification is introduced by the transition to summation over only the reciprocal-lattice vectors K. Indeed, using (2.2), we can easily obtain

$$E^{(2)} = -\frac{\Omega}{2}\sum_{\mathbf{K}\neq 0}\frac{\pi(\mathbf{K})}{\varepsilon(\mathbf{K})}|V_{\mathbf{K}}|^2|S(\mathbf{K})|^2, \quad (2.15)$$

$$E^{(n)} = \Omega\sum_{\mathbf{K}_1, \ldots, \mathbf{K}_n \neq 0}\frac{\Lambda^{(n)}(\mathbf{K}_1, \ldots, \mathbf{K}_n)}{\varepsilon(\mathbf{K}_1)\ldots\varepsilon(\mathbf{K}_n)}V_{\mathbf{K}_1}\ldots V_{\mathbf{K}_n}\times$$
$$\times S(\mathbf{K}_1)\ldots S(\mathbf{K}_n)\Delta(\mathbf{K}_1+\ldots+\mathbf{K}_n) \quad (n>2); \quad (2.16)$$

we present here the results for the general case, and accordingly (2.2) gives rise to the structure factor

$$S(\mathbf{q}) = \frac{1}{\nu}\sum_s \exp(i\mathbf{q}\boldsymbol{\rho}_s). \quad (2.17)$$

The summation in this factor is over all ν ions in the unit cell with relative coordinates $\boldsymbol{\rho}_s$. From the form of (2.16) we can easily understand now that the expansion for the electron energy of a static lattice, starting with n = 2, is indeed a series in the small parameter V_K/ϵ_F.

In concluding this chapter, we note that the employed perturbation theory is in fact approximate, since the coherent restructuring of the electron spectrum near the Brillouin-zone boundaries is taken into account in this theory only approximately. However, as shown by a well known analysis[58], the characteristics integrated over the electron spectrum are determined by this method with high accuracy. It appears that this result is quite general for "good" nontransition metals.

3. DYNAMICAL MATRIX

We proceed now to determine the phonon spectrum in a metal. To this end we recognize that, in accordance with the adiabatic approximation, the role of the potential energy in the vibrational problem for a metal is played by the quantity (see (1.3))

$$U(\mathbf{R}) = U_i(\mathbf{R}) + E_e(\mathbf{R}), \quad (3.1)$$

where $U_i(\mathbf{R})$ is the potential energy of the ion lattice (which is immersed in a compensating homogeneous negative background), and $E_e(\mathbf{R})$ is the ground-state energy of the electron system, obtained as a function of the ion coordinates. We find first the equilibrium positions of the nuclei, corresponding to (3.1). They are given by the stationarity condition and correspond, for the s-th ion in the m-th unit cell, to the requirement

$$\left(\frac{\partial U(\mathbf{R})}{\partial \mathbf{R}_{ms}}\right)_0 = 0. \quad (3.2)$$

The contribution of the indirect inter-pion interaction to this condition is obtained directly from (2.5):

$$\left(\frac{\partial E^{(n)}}{\partial \mathbf{R}_{ms}}\right)_0 = -\frac{n}{N}\Omega\sum_{\mathbf{K}_1, \ldots, \mathbf{K}_n}\mathbf{K}_n\Gamma^{(n)}(\mathbf{K}_1, \ldots, \mathbf{K}_n)V_{\mathbf{K}_1}\ldots$$
$$\ldots V_{\mathbf{K}_n}\operatorname{Im}[S(\mathbf{K}_1)\ldots S(\mathbf{K}_{n-1})\exp(i\mathbf{K}_n\boldsymbol{\rho}_s)]; \quad (3.3)$$

we have used here the fact that $V_{-K} = V_K$, as well as the symmetry relations for the many-pole functions. The obtained condition does not depend on the number of unit cell, as should be the case. In the case of monatomic crystals (Bravais lattice) (3.3) vanishes identically. In a lattice with two atoms per unit cell, Eq. (3.3) vanishes identically only if the displacement of the same atom changes the space group of the lattice symmetry. (It does not vanish, for example, for a bismuth-type structure in the case of a displacement along the trigonal axis.) In the general case only the total force acting on the ion vanishes. The condition (3.2) is in fact an equation for determining the equilibrium value of ρ_s for the atoms inside the unit cell.

To consider the vibrational problem in the harmonic approximation, it is now necessary to find the force matrix (see, e.g., [5,6]), defined relative to the equilibrium position (2.2):

$$(A)^{\alpha\beta}_{ms,\ m's'} = \frac{\partial^2 U}{\partial R^{\alpha}_{ms}\,\partial R^{\beta}_{m's'}} \tag{3.4}$$

(the superscripts denote from now on Cartesian coordinates).

The contribution made to (3.4) by an ionic lattice with pure Coulomb interaction (U_i) is of standard form. The indirect interaction corresponding to E_e, in accordance with (2.4) and (2.5), can be again represented in the form of a series in powers of the electron-ion interaction. This series, as can be easily seen, begins with n = 2, and its general term can be written in the following form ((ms) ≠ (m's')):

$$(A^{(n)})^{\alpha\beta}_{ms,\ m's'} = -n(n-1)\frac{\Omega}{N^2}\sum_{\mathbf{q}_1,\ \mathbf{q}_2,\ \mathbf{K}_3,\ \ldots,\ \mathbf{K}_n}\Gamma^{(n)}(\mathbf{q}_1,\ \mathbf{q}_2,\ \mathbf{K}_3,\ \ldots,\ \mathbf{K}_n)$$
$$\times q_1^{\alpha}q_2^{\beta}V_{\mathbf{q}_1}V_{\mathbf{q}_2}V_{\mathbf{K}_3}\ldots V_{\mathbf{K}_n}\exp\left(i\mathbf{q}_1(\mathbf{R}^{(0)}_m-\mathbf{R}^{(0)}_{m'})+i\mathbf{q}_1\boldsymbol{\rho}_s+i\mathbf{q}_2\boldsymbol{\rho}_{s'}\right)S(\mathbf{K}_3)\ldots$$
$$\ldots S(\mathbf{K}_n)\,\Delta(\mathbf{q}_1+\mathbf{q}_2+\mathbf{K}_3+\ldots+\mathbf{K}_n). \tag{3.5}$$

This yields automatically, for the matrix with ms = m's', the relation

$$(A^{(n)})^{\alpha\beta}_{ms,\ ms} = -\sum_{m's'(\neq ms)}(A^{(n)})^{\alpha\beta}_{ms,\ m's'}, \tag{3.6}$$

which is valid separately for each n and is actually the consequence of translational symmetry, which is taken into account in the expansion (2.4), in the form of the exact momentum-conservation law in each term of (2.5). (We have used for the ion equilibrium coordinate the notation $\mathbf{R}^{(0)}_{ms} = \mathbf{R}^{(0)}_{ms} + \boldsymbol{\rho}_s$). For the first term of the series in (3.5) we obtain the expression

$$(A^{(2)})^{\alpha\beta}_{ms,\ m's'} = -\frac{\Omega}{N^2}\sum_{\mathbf{q}} q^{\alpha}q^{\beta}\,|V_{\mathbf{q}}|^2\,\frac{'\pi(\mathbf{q})}{\varepsilon(\mathbf{q})}\,e^{i\mathbf{q}(\mathbf{R}^{(0)}_{ms}-\mathbf{R}^{(0)}_{m's'})}. \tag{3.7}$$

The elements of this matrix depend thus only on the distance between the ions and correspond to axial symmetry, thus reflecting the central character of the indirect interaction between the two ions in $E^{(2)}$. The ionic contribution to the force matrix has obviously the same symmetry. Therefore, if we discard the remaining terms of the series, the total force matrix in the metal will also have axial symmetry.

However, the next terms in (3.5) lead already to the appearance of a force matrix of more general form with constraints imposed only by the spatial symmetry group of the crystal, which would correspond in the general theory to the existence of covalent forces. Formally this is connected with the fact that at n > 2 the expression (3.5) depends not only on the coordinate of the ion, but also on the structure of the crystal, via the summation over the reciprocal-lattice vectors (the latter are missing only at n = 2). Physically, the appearance of such terms is due to the existence of unpaired indirect interaction between the ions. This question will be considered in greater detail in Chap. 10.

Knowing the force matrix and using the standard procedure, we can immediately obtain the dynamic matrix, diagonalization of which yields the phonon spectrum:

$$D^{\alpha\beta}_{ss'}(\mathbf{q})\,e^{\beta}_{s'}(\mathbf{q}) = \omega^2 e^{\alpha}_{s}(\mathbf{q}), \tag{3.8}$$

$$D^{\alpha\beta}_{ss'}(\mathbf{q}) = \frac{1}{M}\sum_{m'}(A)^{\alpha\beta}_{ms,\ m's'}e^{-i\mathbf{q}(\mathbf{R}^{(0)}_{m's'}-\mathbf{R}^{(0)}_{ms})}. \tag{3.9}$$

Taking into account the translational symmetry, it is convenient to introduce beforehand, for each contribution, the definition

$$D^{\alpha\beta}_{ss'}(\mathbf{q}) = \bar{D}^{\alpha\beta}_{ss'}(\mathbf{q}) - \delta_{ss'}\sum_{s''\neq s'}{}'\,\bar{D}^{\alpha\beta}_{ss''}(0).$$

Then

$$D^{\alpha\beta}_{ss'}(\mathbf{q}) = D^{\alpha\beta}_{iss'}(\mathbf{q}) + D^{\alpha\beta}_{css'}(\mathbf{q}) = D^{\alpha\beta}_{iss'}(\mathbf{q}) + \sum_{n\geqslant 2}{}'\,D^{\alpha\beta}_{(n)ss'}(\mathbf{q}). \tag{3.10}$$

For the ionic contribution we have here

$$\bar{D}^{\alpha\beta}_{iss'}(\mathbf{q}) = \frac{\Omega_0}{Mv}\sum_{\mathbf{K}}(\mathbf{q}+\mathbf{K})^{\alpha}(\mathbf{q}+\mathbf{K})^{\beta}\frac{4\pi z^2e^2}{|\mathbf{q}+\mathbf{K}|^2\Omega_0^2}\,e^{i\mathbf{K}(\boldsymbol{\rho}_s-\boldsymbol{\rho}_{s'})} \tag{3.11}$$

and for the electronic contribution we have

$$\bar{D}^{\alpha\beta}_{(n)ss'}(\mathbf{q}) = \Omega_0\frac{n(n-1)}{Mv}\sum_{\mathbf{K}_1,\ \ldots,\ \mathbf{K}_n}{}'\,(\mathbf{q}+\mathbf{K}_1)^{\alpha}(\mathbf{q}+\mathbf{K}_2)^{\beta}\times$$
$$\times\,\Gamma^{(n)}(\mathbf{q}+\mathbf{K}_1,\ -\mathbf{q}-\mathbf{K}_2,\ \mathbf{K}_3,\ \ldots,\ \mathbf{K}_n)\,V_{\mathbf{q}+\mathbf{K}_1}V_{-(\mathbf{q}+\mathbf{K}_2)}V_{\mathbf{K}_3}\ldots V_{\mathbf{K}_n}$$
$$\times\,e^{i(\mathbf{K}_1\boldsymbol{\rho}_s-\mathbf{K}_2\boldsymbol{\rho}_{s'})}S(\mathbf{K}_3)\ldots S(\mathbf{K}_n)\,\Delta(\mathbf{K}_1-\mathbf{K}_2+\mathbf{K}_3+\ldots+\mathbf{K}_n). \tag{3.12}$$

Let us analyze the obtained expression. The most essential fact is that the character of the expansion of D_e in powers of the electron-ion interaction differs in principle from the corresponding series for the static electron energy E_e. Indeed, each term of this expansion contains two factors V_q, in the general case at arbitrary values of q, whereas in the terms of the series for the energy there are contained the Fourier components only at $\mathbf{q} = \mathbf{K} \neq 0$. However, the statement of the presence of a small parameter V_K/ϵ_F, which corresponds to the pseudopotential theory, is by far not equivalent to the statement that the potential is small in general. To the contrary, it is easily seen that at small momentum transfers the electron interaction is far from small and

$$\left(\frac{1}{\varepsilon_P}\frac{V_{\mathbf{q}}}{\varepsilon(\mathbf{q})}\right)_{\mathbf{q}\to 0}\sim 1 \tag{3.13}$$

(we have introduced here in explicit form the dielectric constant $\epsilon(\mathbf{q})$, recognizing that according to (2.12) the expansion is carried out precisely in terms of this ratio).

To determine also the static energy of the phonons at the same accuracy it is necessary therefore to take into account different numbers of terms in the series. Thus, if the energy is accurate to $(V_K/\epsilon_F)^2$, it suffices to take into account only the term (2.15) with n = 2, whereas in the series for D_e it is necessary here, in general, to take into account terms with n = 3 and n = 4 (at n = 5, the corresponding terms in the dynamical matrix are of order of smallness not lower than $(V_K/\epsilon_F)^3$).

The foregoing result is quite general. The presence of a small parameter makes it possible to express all the quantities integrated over the electron spectrum in the metal in the form of a series in V_K/ϵ_F, but the

higher the derivative of the energy with respect to the ion coordinates in the problem, the more terms of this series must be taken into account (this must be taken into consideration, for example, when anharmonicity is considered).

Let us find the dynamical matrix, bearing this circumstance in mind, and confining ourselves to the accuracy $(V_K/\epsilon_F)^2$. For the region of small q, the situation is obvious, and together with the term $D_{(2)}$ we should retain in the term with n = 3 also the contributions with K_1 or K_2, which are equal to zero, and in the term with n = 4 we should retain the contributions with $K_1 = K_2 = 0$. Then

$$\bar{D}^{\alpha\beta}_{ss'} = \frac{1}{Mv}\sum_K (q+K)^\alpha (q+K)^\beta e^{iK(Q_s - Q_{s'})}\varphi(q+K) + \\ + \frac{6\Omega_0}{Mv}\sum_K \{[q^\alpha (q+K)^\beta e^{-iKQ_{s'}} S(K) + q^\beta (q+K)^\alpha e^{iKQ_s} S^*(K)] \\ \times V_K V_{-(q+K)} V_q \Gamma^{(3)}(q, -q, -K, K) + \\ + 2q_\alpha q_\beta |V_q|^2 |V_K|^2 |S(K)|^2 \Gamma^{(4)}(q, -q, K, K)\}. \quad (3.14)$$

where we have introduced the function

$$\varphi(q) = \frac{4\pi z^2 e^2}{q^2 \omega_0} - \Omega_0 \frac{|V_q|^2 \pi(q)}{\varepsilon(q)}. \quad (3.15)$$

In expression (3.14), the first term is the dynamical matrix D_p corresponding to pair interaction—the direct Coulomb interaction and the indirect interaction due to $E^{(2)}$. (In the $(V_K/\epsilon_F)^3$ approximation, the increments to the pair interaction are contained in $E^{(3)}$; see Chap. 10.) The remaining terms in (3.14) correspond to the unpaired interaction, and are of the same order with the pair interaction.

At noticeable q comparable with the limiting momentum of the phonons, each succeeding term in the expansion of D_e (see (3.10)) contains an extra power of the small parameter, starting in fact already with n = 3. One can therefore hope for a rapid convergence of the series and for the pair term to be singled out at large q. There is, however, a circumstance that makes the allowance for $D_{(3)}$ quite essential in the entire phase region. The point is that in most cases, especially in polyvalent metals, a very strong cancellation of the direct and indirect interactions takes place in D_p [16], and the contribution $D_{(3)}$ should be compared not with $D_{(2)}$, but precisely with D_p. Thus, allowance for at least $D_{(3)}$ in entire phase space is not only of principal character (symmetry), but also of purely quantitative character. We note that the approximation (3.14) is valid only at small q. At large q, the remaining terms in (3.12) become of the same order as the unpaired contribution to (3.14); therefore, in particular, (3.14) does not satisfy the condition D(q + K) = D(q) of periodicity in reciprocal space. For this reason, it is necessary to use the general expression (3.12) at large q.

In concluding this chapter let us dwell briefly on another possible method of determining the dynamic oscillation matrix, based on the use of the dielectric formalism for periodic structures. The corresponding results are easiest to obtain if, starting from the validity of the adiabatic approximation, one uses the Hamiltonian (2.1), expanding the term of the electron-ion interaction in the displacements of the ions. One can pose next the problem of determining the change produced in the energy of the electron system by a displacement wave with a definite wave vector q. In the harmonic approximation we need to find the energy only in second order in the displacement. The problem is then formally perfectly equivalent to the problem of the dielectric constant and its exact definition (see [4,31]).

We choose as the basis $|n\rangle$ the exact wave functions of the total Hamiltonian of a periodic static lattice with allowance for electron-electron interaction. In this basis, the reaction of the medium on the displacement wave is obtained directly, and for the electronic dynamical matrix in a monatomic crystal we obtain the expression [10,11,32]

$$D_e^{\alpha\beta}(q) = \frac{1}{M\Omega_0}\sum_{K,K'} (q+K)^\alpha (q+K')^\beta V_{q+K} V_{-(q+K')} \chi(q+K, -q-K'); \quad (3.16)$$

here

$$\chi(q, q') = \sum_n \frac{\langle 0|\rho_q^*|n\rangle\langle n|\rho_{-q'}|0\rangle}{E_0 - E_n} \quad (3.17)$$

is the static function of the density—density reaction (see [4]) and ρ_q are the Fourier components of the electron-density operator.

In the RPA approximation, a similar expression was first obtained by Sham [12]. The result (3.16) is in principle quite general. In particular, it is applicable also to transition metals and dielectrics, if the electronic and ionic subsystems are suitably separated. The simplicity of this expression, however, is quite illusory and it is impossible to use it in an exact initial form.

If the exact multiparticle wave function $|0\rangle$ is represented in the form of a perturbation-theory series in the electron-ion interaction in a periodic lattice, then it can easily be seen that (3.17) is described by an aggregate of the many-point diagrams represented in Fig. 1, where the two external-field lines have momenta q and q′, and the remaining ones have momenta equal to the reciprocal-lattice vectors. We shall sum with respect to the latter with the corresponding factors V_K. The coefficients of each diagram with n points turns out to be equal to (n − 1).

Comparing this result with (3.12), we verify directly that the dynamic vibration matrix obtained in this case from (3.16) coincides exactly with the result given above in this section [15].

Thus, if we use perturbation theory in terms of the electron-ion interaction, then (3.16) does not lead to a new result (see also [32]). In the initial form, however, it is more general, since it incorporates in principle a coherent restructuring of the electron spectrum near the boundaries of the Brillouin zone where, strictly speaking, expansion in the electron-ion interaction is not valid.

As already noted in Chap. 2, there exists also a "field" method of determining the vibrational spectrum, based on a renormalization of correctly chosen "bare" particles and using a simple vertex for the electron-phonon interaction. The problem reduces in this case to a solution of a system of Dyson's equations. It can be shown that if the possibility of rescattering by a static lattice is correctly taken into account, the result in final form also coincides with (3.12).

4. LONG-WAVE PHONONS IN A METAL

We begin a more detailed consideration with an analysis of sound in a metal, confining ourselves in this stage, for simplicity, to the case of one atom per unit cell and to an accuracy of order $(V_K/\epsilon_F)^2$. To this end, we go over to the region of extremely long waves and expand

(3.14) in powers of q. The expansion of the pair dynamical matrix D_p (the first term in (3.14)) can be easily obtained by recognizing that (3.15) leads to the expression

$$\varphi(\mathbf{q}\to 0)=\frac{z^2}{\pi(0)\Omega_0}+\frac{2bz}{\Omega_0}\equiv\varphi(0). \tag{4.1}$$

We then obtain

$$D_p^{\alpha\beta}(\mathbf{q})=\frac{6}{M}\mathbf{q}^\alpha\mathbf{q}^\beta\varphi(0)+\frac{1}{M}\sum_{\mathbf{K}\neq 0}\Big[\mathbf{q}^\alpha\mathbf{q}^\beta\varphi(\mathbf{K})-(\mathbf{q}^\alpha\mathbf{K}^\beta+\mathbf{q}^\beta\mathbf{K}^\alpha)\mathbf{q}^\gamma\frac{\partial\varphi(\mathbf{K})}{\partial\mathbf{K}^\gamma}+\frac{1}{2}\mathbf{q}^\gamma\mathbf{q}^\delta\mathbf{K}^\alpha\mathbf{K}^\beta\frac{\partial^2\varphi(\mathbf{K})}{\partial\mathbf{K}^\gamma\partial\mathbf{K}^\delta}\Big]. \tag{4.2}$$

The three-particle contribution to the dynamical matrix is also obtained directly from (3.14). It is convenient here to introduce immediately irreducible many-pole functions in accordance with (2.12):

$$D_{(3)}^{\alpha\beta}(\mathbf{q})=-\frac{6}{M}\frac{z}{\pi(0)}\sum_{\mathbf{K}\neq 0}\Big\{2\mathbf{q}^\alpha\mathbf{q}^\beta\Big(\frac{V_\mathbf{K}}{\varepsilon(\mathbf{K})}\Big)^2\Lambda^{(3)}(0,\mathbf{K},-\mathbf{K})-(\mathbf{q}^\alpha\mathbf{K}^\beta+\mathbf{q}^\beta\mathbf{K}^\alpha)\mathbf{q}^\gamma\Big[\Big(\frac{V_\mathbf{K}}{\varepsilon(\mathbf{K})}\Big)\frac{\partial}{\partial\mathbf{K}^\gamma}\frac{V_\mathbf{K}}{\varepsilon(\mathbf{K})}\Lambda^{(3)}(0,\mathbf{K},-\mathbf{K})+\Big(\frac{V_\mathbf{K}}{\varepsilon(\mathbf{K})}\Big)^2\Big(\frac{\partial}{\partial\mathbf{q}^\gamma}\Lambda^{(3)}(\mathbf{q},-\mathbf{q},-\mathbf{K},\mathbf{K})\Big)_{\mathbf{q}\to 0}\Big]\Big\}. \tag{4.3}$$

In analogy, for the four-particle contribution we have

$$D_{(4)}^{\alpha\beta}(\mathbf{q})=\frac{12}{M\Omega_0}\Big(\frac{z}{\pi(0)}\Big)^2\mathbf{q}^\alpha\mathbf{q}^\beta\sum_{\mathbf{K}\neq 0}\Big(\frac{V_\mathbf{K}}{\varepsilon(\mathbf{K})}\Big)^2\Lambda^{(4)}(0,0,\mathbf{K},-\mathbf{K}). \tag{4.4}$$

In the derivation of (4.3) and (4.4) we have used the fact that, in accordance with (2.6) and (2.11),

$$\Big(\frac{V_\mathbf{q}}{\varepsilon(\mathbf{q})}\Big)_{\mathbf{q}\to 0}\to-\frac{z}{\pi(0)\Omega_0},\quad\Big(\frac{\partial}{\partial\mathbf{q}}\frac{V_\mathbf{q}}{\varepsilon(\mathbf{q})}\Big)_{\mathbf{q}\to 0}\to 0.$$

As seen from the obtained expressions, to determine completely the sound velocities or the elastic moduli we must determine the explicit forms of $\Lambda^{(3)}$ and $\Lambda^{(4)}$ for the particular case when one or two of the arguments in them are equal to zero. It turns out that this problem can be solved in general form and a number of exact relations similar to the Ward identities and valid for an arbitrary normal Fermi surface can be established for these functions[17]. A diagramatic derivation of these relations is based on the technique of skeleton diagrams and on the differentiation of the "thick" electronic Green's functions with respect to the chemical potential, which is equivalent to introducing an additional vertex with an incoming zero momentum. The details can be found in our earlier paper[17], where the following system of identities was established:

$$\varepsilon(0)\,\Gamma^{(n+1)}(\mathbf{q}_1,\ldots,\mathbf{q}_n,0)=-\frac{1}{n+1}\frac{d\Gamma^{(n)}(\mathbf{q},\ldots,\mathbf{q}_n)}{d\mu}; \tag{4.5}$$

the divergence of $\epsilon(0)$ as $\mathbf{q}\to 0$ is compensated here by the corresponding factor in $\Gamma^{(n+1)}$. For $n>2$ it is therefore convenient to rewrite (4.5) by introducing the irreducible functions (2.2):

$$\frac{\Lambda^{(n+1)}(\mathbf{q}_1,\ldots,\mathbf{q}_n,0)}{\varepsilon(\mathbf{q}_1)\ldots\varepsilon(\mathbf{q}_n)}=-\frac{1}{n+1}\frac{d\Gamma^{(n)}(\mathbf{q}_1,\ldots,\mathbf{q}_n)}{d\mu}. \tag{4.6}$$

For the particular cases needed by us we obtain, taking (2.10) into account,

$$\frac{\Lambda^{(3)}(0,\mathbf{K},-\mathbf{K})}{[\varepsilon(\mathbf{K})]^2}=\frac{1}{6}\frac{d}{d\mu}\frac{\pi(\mathbf{K})}{\varepsilon(\mathbf{K})}. \tag{4.7}$$

In the determination of $\Lambda^{(4)}(0,0,\mathbf{K},-\mathbf{K})$ it must be borne in mind that we are interested in a definite limit, namely $\Lambda^{(4)}(\mathbf{q},-\mathbf{q},\mathbf{K},-\mathbf{K})$. As can be easily understood, owing $\mathbf{q}\to 0$ to the electroneutrality, definite diagrams drop out of this expression, so that when (4.5) is repeatedly differentiated with respect to μ one must not differentiate $\epsilon(0)$.

As a result we obtain

$$\frac{\Lambda^{(4)}(0,0,\mathbf{K},-\mathbf{K})}{(\varepsilon(\mathbf{K}))^2}=-\frac{1}{24}\frac{d^2}{d\mu^2}\frac{\pi(\mathbf{K})}{\varepsilon(\mathbf{K})}. \tag{4.8}$$

With the aid of (4.5) we can establish one more important relation. We consider the case n = 2. Then, in accordance with (2.8) and (2.10), we obtain

$$\pi(0)=\frac{dn_0}{d\mu}. \tag{4.9}$$

This result, usually obtained in Fermi-liquid theory by another method[4], is thus the simplest particular case of (4.5). It enables us to transform the differentiation with respect to the electron density:

$$\frac{\Lambda^{(3)}(0,\mathbf{K},-\mathbf{K})}{(\varepsilon(\mathbf{K}))^2}=\frac{\pi(0)}{6}\frac{d}{dn_0}\frac{\pi(\mathbf{K})}{\varepsilon(\mathbf{K})}. \tag{4.10}$$

With the aid of (4.9) we can also transform (4.8). It should be noted here that $\Lambda^{(n)}$ in the foregoing expressions actually means $\Lambda^{(n)}_\Omega$ (see (2.13))—the two simply coincide at n = 3. To determine the total four-pole diagram it is necessary, on the other hand, to add to (4.8) the contribution $\Lambda^{(4)}_\mu$ (2.14). Putting in it $\mathbf{q}_2=0$, we obtain ultimately after simple transformations

$$\frac{\Lambda^{(4)}(\mathbf{K},-\mathbf{K},0,0)}{(\varepsilon(\mathbf{K}))^2}=-\frac{1}{24}(\pi(0))^2\frac{d^2}{dn^2}\frac{\pi(\mathbf{K})}{\varepsilon(\mathbf{K})}. \tag{4.11}$$

We can finally obtain also an identity for the differentiation of the irreducible multipoles[17]

$$\Big(\frac{\partial}{\partial q^\alpha}\Lambda^{(3)}(\mathbf{q},-\mathbf{q},\mathbf{K},-\mathbf{K})\Big)_{\mathbf{q}\to 0}=\frac{1}{2}\frac{\partial}{\partial\mathbf{K}^\alpha}\Lambda^{(3)}(0,\mathbf{K},-\mathbf{K}). \tag{4.12}$$

Thus, expressions (4.10)—(4.12) show that the dynamic matrix at small q, and consequently also the speeds of sound, depend on the properties of the electron liquid only in terms of the polarizability $\pi(\mathbf{q})$ and its derivatives.

It is convenient to carry out the analysis of the sound velocities in the language of the dynamic elastic moduli. To this end, we introduce the notation of Born and Huang[5]

$$D^{\alpha\beta}(\mathbf{q})=\frac{\Omega_0}{M}[\alpha\beta,\gamma\delta]\mathbf{q}^\gamma\mathbf{q}^\delta \tag{4.13}$$

and use the general expression for the elastic moduli of the monatomic crystal

$$c_{\alpha\beta\gamma\delta}=[\alpha\gamma,\beta\delta]+[\gamma\beta,\alpha\delta]-[\gamma\delta,\alpha\beta]. \tag{4.14}$$

Comparison of (4.13) with (4.2) and (4.3) makes it possible to determine the value of the moduli $c_{\alpha\beta\gamma\delta}$ for an arbitrary crystal. We confine ourselves here, for simplicity, to the case of cubic symmetry. We then get for the elastic modulus $c_{11}=c_{xxxx}$, corresponding to a longitudinal sound velocity with q along the edge of the cube, using the identities given above,

$$c_{11}=\frac{n_0^2}{\pi(0)}-\frac{2bn_0}{\Omega_0}+\frac{1}{\Omega_0}\sum_{\mathbf{K}\neq 0}\Big[\varphi(\mathbf{K})-2\mathbf{K}_x\frac{\partial\varphi(\mathbf{K})}{\partial\mathbf{K}_x}+\frac{1}{2}(\mathbf{K}_x)^2\frac{\partial^2\varphi(\mathbf{K})}{\partial\mathbf{K}_x^2}\Big]-n_0\sum_{\mathbf{K}\neq 0}\Big[2|V_\mathbf{K}|^2\frac{\partial}{\partial n_0}\frac{\pi(\mathbf{K})}{\varepsilon(\mathbf{K})}+\frac{1}{3}\mathbf{K}^\alpha\frac{\partial}{\partial\mathbf{K}^\alpha}\Big(|V_\mathbf{K}|^2\frac{\partial}{\partial n_0}\frac{\pi(\mathbf{K})}{\varepsilon(\mathbf{K})}\Big)+\frac{1}{2}n_0|V_\mathbf{K}|^2\frac{\partial^2}{\partial n_0^2}\frac{\pi(\mathbf{K})}{\varepsilon(\mathbf{K})}\Big]. \tag{4.15}$$

Recognizing that neither direct ion-ion interaction nor the "bare" electron-ion interaction depends on the electron density, we can rewrite (4.15) also in the following convenient form, introducing the pair-interaction function $\varphi(\mathbf{q})$ (3.15):

$$c_{11}=\frac{\varphi(0)}{\Omega_0}+\frac{1}{\Omega_0}\sum_{\mathbf{K}\neq 0}\Big[\varphi(\mathbf{K})-2\mathbf{K}_x\frac{\partial\varphi(\mathbf{K})}{\partial\mathbf{K}_x}+\frac{1}{2}\mathbf{K}_x^2\frac{\partial^2\varphi(\mathbf{K})}{\partial\mathbf{K}_x^2}\Big]+\frac{1}{\Omega_0}\sum_{\mathbf{K}\neq 0}\Big[2n_0\frac{\partial\varphi(\mathbf{K})}{\partial n_0}+\frac{1}{3}n_0\mathbf{K}^\alpha\frac{\partial^2\varphi(\mathbf{K})}{\partial\mathbf{K}^\alpha\partial n_0}+\frac{1}{2}n_0^2\frac{\partial^2\varphi(\mathbf{K})}{\partial n_0^2}\Big]. \tag{4.16}$$

Expressions (4.15) and (4.16) determine the square of the longitudinal velocity of sound in a metal, accurate to $(V_K/\epsilon_F)^2$ inclusive. Its analysis is very instructive from the physical point of view. The first two terms in (4.15) (the first term in (4.16)) describe the contribution from a homogeneous continuous medium and coincide with the known result of Bardeen and Pines[34]. The first of the terms corresponds to a plasma with pointlike ions, and if we assume for $\pi(0)$ the value obtained in the self-consistent-field method or in the random-phase method, $\pi(0) = (3/2)\, n_0/\epsilon_F$, then it yields the longitudinal sound velocity first obtained by Bohm and Staver[35]. However, it is precisely the second term in (4.15), which is connected with the non-pointlike character of the ions, which plays a very important role in the formation of longitudinal sound in a metal, and as a rule exceeds the first term.

The inhomogeneity of the medium becomes manifest in the presence of the third and fourth terms in (4.15), which contain contributions from the direct interaction of the discrete-lattice ions (the first term in $\varphi(\mathbf{K})$ and its derivatives), and also from the indirect inter-ion interaction via the conduction electrons. An important factor in this case is that in longitudinal sound the contribution of the multi-ion forces (the last terms in (4.15) and (4.16)) in the structurally-dependent part does not contain small quantities and turns out to be of the same order as the contribution from the indirect pair interaction. It follows from this, in particular, that any representation based only on the paired dynamical matrix D_p is certain to describe incorrectly the long-wave region of the known spectrum.

Comparing (4.13) with (4.2)—(4.4) and using (4.14), it is easy likewise to determine the shear moduli corresponding to transversely-polarized sound. With the same accuracy $(V_K/\epsilon_F)^2$ we have

$$c_{44} = \frac{1}{2\Omega_0} \sum_{\mathbf{K}\neq 0} (\mathbf{K}^x)^2 \frac{\partial^2 \varphi(\mathbf{K})}{\partial (\mathbf{K}^y)^2}, \qquad (4.17)$$

$$c' = \frac{c_{11}-c_{12}}{2} = \frac{1}{4\Omega_0} \sum_{\mathbf{K}\neq 0} \left[(\mathbf{K}^x)^2 \frac{\partial^2 \varphi(\mathbf{K})}{\partial (\mathbf{K}^x)^2} + (\mathbf{K}^y)^2 \frac{\partial^2 \varphi(\mathbf{K})}{\partial (\mathbf{K}^y)^2} - 2\mathbf{K}^x\mathbf{K}^y \frac{\partial^2 \varphi(\mathbf{K})}{\partial \mathbf{K}^x\, \partial \mathbf{K}^y} \right]. \qquad (4.18)$$

It follows from these expressions that in an approximation in which terms of order $(V_K/\epsilon_F)^2$ are retained, the shear moduli are determined entirely by the pair interaction and do not contain a contribution from the multi-ion forces. The contribution of the latter, just as in the energy of the static lattice, begins with terms of order $(V_K/\epsilon_F)^3$. It should be noted, however, that the role of these expansion terms can turn out to be quite significant from the quantitative point of view. The reason is that the transverse sound velocities, unlike the longitudinal one (4.15) or (4.16), do not contain terms corresponding to a continuous medium (K = 0). Therefore, if the electronic and ionic contributions to (4.17) and (4.18) are comparable in magnitude, then allowance for the third-order terms will yield an important first-order correction to the total value of the elastic modulus. This circumstance becomes particularly important when the velocity of the surface sound is small. There are known cases, for example in tin[15] or in zinc[16], when the ionic lattice is in general unstable with respect to certain transverse oscillations and becomes stable only as a result of the electronic contribution. In this case the multi-ion terms can play even the decisive role.

In the opposite case, when the electronic contribution to (4.17) or (4.18) is small in comparison with the ionic contribution, owing to the particular smallness of the parameter V_K/ϵ_F, as is the case, for example, in metallic sodium, the transverse sound is determined practically entirely by the ion lattice.

In metals with several atoms per unit cell, there appear also additional optical modes that can also be analyzed in the long-wave limit. Let us consider by way of example a metal with two identical atoms per unit cell, and let the symmetry be high enough to make the matrix (3.9) at $\mathbf{q} = 0$ diagonal in the Cartesian indices. This gives rise to decay into three independent optical modes with polarizations along the selected axes. Using (3.14), we obtain for the limiting frequencies, again accurate to $(V_K/\epsilon_F)^2$ inclusive,

$$\omega_\alpha^2(\mathbf{q}=0) = -\frac{2}{M} \sum_{\mathbf{K}\neq 0} (\mathbf{K}^\alpha)^2 \varphi(\mathbf{K}) \cos(\mathbf{K}\rho) \quad (\alpha = x, y, z). \qquad (4.19)$$

This expression is similar in structure to expressions (4.17) and (4.18) for the shear moduli. Here, too, there is no homogeneous contribution (K = 0), and the multi-ion forces become manifest only in terms of order $(V_K/\epsilon_F)^3$ and higher.

As a result, all the considerations advanced above remain in force. In particular, all available metals are frequently characterized by a strong mutual cancellation of the electron and ion contributions in (4.19), at which the role of the multi-ion interaction turns out to be quite appreciable (see[15,16]).

5. THE PROBLEM OF COMPRESSIBILITY

One of the interesting problems in the theory of metals is the question of the relation between the dynamic compressibility, i.e., that determined from the speed of sound, and the static compressibility, which is determined from the energy:

$$\frac{1}{\varkappa} = B = \Omega \left(\frac{\partial^2 E}{\partial \Omega^2} \right)_N \qquad (5.1)$$

(B is the bulk modulus). If we analyze the customarily employed expressions for the energy and the dynamic matrix, which are equivalent to taking pair interaction into account, i.e., if we retain in (2.4) and (3.10) only terms with n = 2, then the expressions obtained for the compressibility do not agree. At first glance, from the formal point of view, this may seem natural for a system in which an important role is played by the electron liquid, since the static compressibility is determined by all the terms of (2.4), whereas the dynamic compressibility is made up only of a part of these terms, those with $n \geq 2$. On the other hand, the dynamic problem in metals is considered at a constant electron density, whereas in the static case there appear in explicit form terms corresponding to the change of the density, and consequently, for example, to the dielectric constant.

However, as shown by a detailed analysis[36], while all the indicated problems do exist, a consistent consideration of multi-ion interaction makes it possible to prove the equality of the static and dynamic compressibilities.

To discuss this problem, we determine first the static compressibility (5.1), and for the sake of simplicity we confine ourselves to lattices with one atom per unit cell (the generalization to an arbitrary case entails no difficulties in principle). To this end we use the expression for the total static energy

$$E = E_i + E_e, \tag{5.2}$$

where E_e is defined in Chap. 2, and for E_i we have

$$E_i = \frac{1}{2} \sum_{m \neq m'} \sum_{\mathbf{q} \neq 0} \frac{4\pi z^2 e^2}{\mathbf{q}^2 \Omega} e^{i\mathbf{q}(\mathbf{R}_m - \mathbf{R}_{m'})} = \frac{1}{2} N \sum_{\mathbf{K} \neq 0} \frac{4\pi z^2 e^2}{\mathbf{K}^2 \Omega_0} - \frac{1}{2} \sum_{\mathbf{q} \neq 0} \frac{4\pi z^2 e^2}{\mathbf{q}^2 \Omega_0}. \tag{5.3}$$

The contribution to the bulk modulus $B^{(0)}$ from the energy $E^{(0)}$ of the homogeneous interacting electron gas can be obtained by recognizing that

$$(\varkappa^{(0)})^{-1} = n_0^2 \frac{d\mu}{dn_0},$$

and by using expression (4.9):

$$B^{(0)} = \frac{n_0^2}{\pi(0)}. \tag{5.4}$$

The contribution from $E^{(1)}$ is obtained from (2.9) directly:

$$B^{(1)} = \frac{2hz}{\Omega_0^2}. \tag{5.5}$$

In the determination of the compressibility connected with the structurally-dependent terms in (5.2), it must be borne in mind that the energy, besides the explicit dependence on the volume, contains also an implicit dependence via the reciprocal-lattice vectors and via the dependence of the polarization operator $\pi(\mathbf{q})$ on the electron-gas density n_0. Accordingly we have[36]

$$\frac{\partial}{\partial \Omega} = \left(\frac{\partial}{\partial \Omega}\right)_{\mathbf{K}, n_0} - \frac{1}{3\Omega} \mathbf{K}^\alpha \left(\frac{\partial}{\partial \mathbf{K}^\alpha}\right)_{\Omega, n_0} - \frac{n_0}{\Omega} \left(\frac{\partial}{\partial n_0}\right)_{\Omega, \mathbf{K}} \tag{5.6}$$

(the differentiation is carried out throughout at constant N).

The form of the second term of (5.6) suggests a similar change in the unit cell with changing volume. In a cubic crystal in the presence of an external homogeneous pressure, this assumption is automatically satisfied. To simplify the exposition, we confine ourselves henceforth to just this case.

We calculate now the contribution made to the compressibility by E_i (5.3) and $E^{(2)}$ (2.15). We first fix the electron density and determine that part of the compressibility which is governed by the first two terms of (5.6). We take into account here the fact that the second term in (5.3) does not depend at all on the volume (on going from summation to integration with respect to $\mathbf{q}$, the quantity Ω appears, but $\Omega/\Omega_0 = N$), while the former depends on Ω also explicitly via $\mathbf{K}$. In addition, we recognize that by definition we have

$$V_{\mathbf{q}} \sim \frac{1}{\Omega_0}.$$

Direct calculation yields therefore

$$B_p^{(2)} = B_i + B_1^{(2)} = \frac{1}{\Omega_0} \sum_{\mathbf{K} \neq 0} \left[\varphi(\mathbf{K}) + \frac{5}{9} \mathbf{K}^\alpha \frac{\partial \varphi(\mathbf{K})}{\partial \mathbf{K}^\alpha} + \frac{1}{18} \mathbf{K}^\alpha \mathbf{K}^\beta \frac{\partial^2 \varphi(\mathbf{K})}{\partial \mathbf{K}^\alpha \partial \mathbf{K}^\beta} \right], \tag{5.7}$$

where $\varphi(\mathbf{K})$ is defined by (3.15). It is easy to see that the contribution from $E^{(2)}$ connected with the change of the electron density n_0 takes the following form:

$$B_{np}^{(2)} = -\sum_{\mathbf{K} \neq 0} \left[\frac{1}{2} n_0^2 |V_{\mathbf{K}}|^2 \frac{\partial^2}{\partial n_0^2} \frac{\pi(\mathbf{K})}{\varepsilon(\mathbf{K})} + 2n_0 |V_{\mathbf{K}}|^2 \frac{\partial}{\partial n_0} \frac{\pi(\mathbf{K})}{\varepsilon(\mathbf{K})} + \frac{1}{3} n_0 \mathbf{K}^\alpha \frac{\partial}{\partial \mathbf{K}^\alpha} \left(|V_{\mathbf{K}}|^2 \frac{\partial}{\partial n_0} \frac{\pi(\mathbf{K})}{\varepsilon(\mathbf{K})} \right) \right]. \tag{5.8}$$

Introducing, as in Chap. 4, the pair interaction $\varphi(\mathbf{q})$ and incorporating all the contributions in the static compressibility, we obtain ultimately

$$B = B^{(0)} + B^{(1)} + B_p^{(2)} + B_{np}^{(2)} = \frac{\varphi(0)}{\Omega_0} + \frac{1}{\Omega_0} \sum_{\mathbf{K} \neq 0} \left[\varphi(\mathbf{K}) + \frac{5}{9} \mathbf{K}^\alpha \frac{\partial \varphi(\mathbf{K})}{\partial \mathbf{K}^\alpha} + \frac{1}{18} \mathbf{K}^\alpha \mathbf{K}^\beta \frac{\partial^2 \varphi(\mathbf{K})}{\partial \mathbf{K}^\alpha \partial \mathbf{K}^\beta} \right] + \frac{1}{\Omega_0} \sum_{\mathbf{K} \neq 0} \left[2n_0 \frac{\partial \varphi(\mathbf{K})}{\partial n_0} + \frac{1}{3} n_0 \frac{\partial^2 \varphi(\mathbf{K})}{\partial n_0 \partial \mathbf{K}^\alpha} + \frac{n_0^2}{2} \frac{\partial^2 \varphi(\mathbf{K})}{\partial n_0^2} \right]. \tag{5.9}$$

Allowance for the next higher term in the expansion of the electron energy would yield a contribution of the order of $(V_K/\epsilon_F)^3$ to the compressibility, and thus (5.9) determines the static compressibility accurate to $(V_K/\epsilon_F)^2$ inclusive. We compare now (5.9) with the expression for the bulk modulus

$$B = \frac{c_{11} + c_{12}}{3}, \tag{5.10}$$

which will be determined with the same accuracy if we use the results (4.16) and (4.18) obtained in the preceding chapter by considering long-wave phonons in the dynamic problem. Direct comparison of all the contributions to the static and dynamic compressibilities shows that both expressions coincide exactly.

A similar proof can be obtained in any order in V_K/ϵ_F. It must be remembered here that, as follows from the preceding chapter, it is necessary to retain each time two more expansion terms in the dynamical matrix than in the corresponding expansion for the energy.

The result is quite nontrivial, inasmuch as in the static approach it turned out to be necessary to take into account the terms $E^{(0)}$, $E^{(1)}$, and $E^{(2)}$ in the expansion (2.4), whereas in the dynamic approach we have the entirely different terms $E^{(2)}$, $E^{(3)}$, and $E^{(4)}$. It is therefore advisable to discuss the situation in somewhat greater detail. The term $E^{(2)}$ in the expansion (2.4) for the energy, if we consider a fixed electron density in conjunction with E_i, describes the effective pair interaction between the ions, and it is natural that the contribution, equivalent to B_p (5.7), to the dynamic compressibility is obtained from the paired part of the dynamic matrix (the second term in (4.2)). However, changing the volume alters not only the distance between the ions, but also the interaction itself, through the change in the electron density. A unique non-paired type of interaction arises between the ions in the metal, although the same type is obtained in the static problem from $E^{(2)}$. This leads to the appearance of the term $B_{np}^{(2)}$ (5.8). It is typical that the equivalent contribution to the dynamic problem is now already connected explicitly with the multi-ion terms of third and fourth order in the electron interaction. It must therefore be emphasized that if no account is taken of the multi-ion interaction, the static and dynamic compressibility cannot be made equal. The quantitative difference between them can be quite appreciable, especially in polyvalent metals, although it can reach also 30% in alkali metals.

The part of the static compressibility corresponding to the continuous medium $B^{(0)} + B^{(1)}$, is also obtained in the dynamic problem from D_p (the first term of (4.2), which does not depend on $\mathbf{K}$), and equality of the corresponding contributions to the compressibility is obtained only when account is taken of relation (4.9). Since this relation is valid only in the exact theory of an interacting electron gas, in which all orders of perturbation theory are taken into account, the quantity $\Omega \partial^2 E^{(0)}/\partial \Omega^2$ does not coincide in general with (5.4), in the approximate theories (for example, a strong deviation from this equality is obtained in the random-phase approximation).

The energy of the electron gas as a functional of the exact Green's function has, as is well known, the stationarity property[33], and is therefore usually determined with a higher accuracy than such a characteristic as the polarizability $\pi(\mathbf{q})$. Therefore to obtain self-consistent results, especially in the analysis of the phonon spectrum of metals, it is necessary to use for $\pi(\mathbf{q})$ representations that satisfy (5.4)[16,37].

6. NATURE OF VIOLATION OF THE CAUCHY RELATIONS IN METALS

As is well known[5], if the interaction between the atoms in the crystal has a paired (central) character, then in the absence of an external pressure the elastic moduli should satisfy the so-called Cauchy relations

$$c_{\alpha\beta\gamma\delta} = c_{\alpha\gamma\beta\delta}.$$

For cubic crystals these reduce to a single relation

$$c_{12} = c_{44}. \tag{6.1}$$

It has been established experimentally, however, that the Cauchy relations are not satisfied in all metals. One possible explanation (in the absence of overlap between the ions) lies in the role of the multi-ion interaction considered above, which leads directly to nonpaired forces. However, certainly there exist metals where the multiparticle forces are small, but the Cauchy relation is violated to full degree. Examples are Na and K, where the measured phonon spectrum[38,39] is very well described in the approximation of a pure pair interaction between ions. The explanation should be sought in the fact that the contribution of the electron liquid to the lattice equilibrium does not reduce merely to a pair interaction between ions. A qualitative explanation of this circumstance can apparently be found in a number of papers, but a complete analysis of the problem was given only recently[36].

From the expressions (4.15)—(4.18), which were obtained above with accuracy to $(V_K/\epsilon_F)^2$, we can write down directly for cubic-symmetry crystals

$$c_{12}-c_{44}=\frac{n_0^2}{\pi(0)}+\frac{2bn_0}{\Omega_0}+\frac{1}{\Omega_0}\sum_{\mathbf{K}\neq 0}\left[\varphi(\mathbf{K})+\frac{1}{3}\mathbf{K}^\alpha\frac{\partial\varphi(\mathbf{K})}{\partial\mathbf{K}^\alpha}\right]$$
$$-\sum_{\mathbf{K}\neq 0}\left[2n_0|V_\mathbf{K}|^2\frac{\partial}{\partial n_0}\frac{\pi(\mathbf{K})}{\varepsilon(\mathbf{K})}+\frac{1}{3}\mathbf{K}^\alpha\frac{\partial}{\partial\mathbf{K}^\alpha}\left(|V_\mathbf{K}|^2\frac{\partial}{\partial n_0}\frac{\pi(\mathbf{K})}{\varepsilon(\mathbf{K})}\right)+\frac{1}{2}n_0^2\frac{\partial^2}{\partial n_0^2}\frac{\pi(\mathbf{K})}{\varepsilon(\mathbf{K})}\right]. \tag{6.2}$$

To introduce the equilibrium condition we now find the general expression for the pressure $P = -\partial E/\partial\Omega$. In accordance with (5.2) and (2.4), we obtain

$$P = P_i + \sum_{n=0}^{\infty} P^{(n)}. \tag{6.3}$$

The pressure produced by a homogeneous interacting electron gas

$$P^{(0)}=-\frac{\partial E^{(0)}}{\partial\Omega},$$

is conveniently expressed in terms of the polarization operator. To this end it is necessary to integrate the reciprocal compressibility (5.4) with respect to the density:

$$P^{(0)}=\frac{1}{2}\frac{n_0^2}{\pi(0)}-\frac{1}{2}\int_0^{n_0}\partial n_0 n_0^2\frac{\partial}{\partial n_0}\frac{1}{\pi(0)}. \tag{6.4}$$

For $P^{(1)}$ we get from (2.9)

$$P^{(1)}=\frac{bz}{\Omega_0^2}. \tag{6.5}$$

The other terms of the series (6.2) can be obtained from the energy by direct application of the operator (5.6). Confining ourselves to the previous accuracy $(V_K/\epsilon_F)^2$ and respectively omitting from (6.3) terms with $n \geq 3$, we obtain ultimately after a number of transformations

$$P=\frac{1}{2}\frac{n_0^2}{\pi(0)}+\frac{bn_0}{\Omega_0}+\frac{1}{2\Omega_0}\sum_{\mathbf{K}\neq 0}\left[\varphi(\mathbf{K})+\frac{1}{3}\mathbf{K}^\alpha\frac{\partial\varphi(\mathbf{K})}{\partial\mathbf{K}^\alpha}\right]$$
$$-\frac{1}{2}\int_0^{n_0}dn_0 n_0^2\frac{\partial}{\partial n_0}\frac{1}{\pi(0)}-\frac{1}{2}n_0\sum_{\mathbf{K}\neq 0}|V_\mathbf{K}|^2\frac{\partial}{\partial n_0}\frac{\pi(\mathbf{K})}{\varepsilon(\mathbf{K})}. \tag{6.6}$$

Now, if we neglect in (6.2) and (6.6) terms that contain the derivatives with respect to the electron density, then $c_{12} - c_{44} = 2P$ and the equilibrium condition $P = 0$ leads immediately to $c_{12} = c_{44}$, i.e., to satisfaction of the Cauchy relation. The presence of derivatives with respect to the density is precisely a reflection of the fact that the picture of the interaction in a metal cannot be adequately described in the language of paired forces.

The equilibrium condition with allowance for all terms in (6.6) leads to the relation

$$c_{12}-c_{44}=\int_0^{n_0}dn_0 n_0^2\frac{\partial}{\partial n_0}\frac{1}{\pi(0)}-\sum_{\mathbf{K}\neq 0}\left[n_0|V_\mathbf{K}|^2\frac{\partial}{\partial n_0}\frac{\pi(\mathbf{K})}{\varepsilon(\mathbf{K})}\right.$$
$$\left.-\frac{1}{3}\mathbf{K}^\alpha\frac{\partial}{\partial\mathbf{K}^\alpha}\left(|V_\mathbf{K}|^2\frac{\partial}{\partial n_0}\frac{\pi(\mathbf{K})}{\varepsilon(\mathbf{K})}+\frac{n_0^2}{2}\frac{\partial^2}{\partial n_0^2}\frac{\pi(\mathbf{K})}{\varepsilon(\mathbf{K})}\right)\right]. \tag{6.7}$$

(The last term can be rewritten also in terms of derivatives of $\varphi(\mathbf{K})$.) This expression demonstrates clearly the presence of two causes of violation of the Cauchy relation in a metal. The first is connected with the nonpaired character of the direct inter-ion interaction, and corresponds to the second term of (6.7) (see the discussion in the preceding chapter). The second cause is the unique role played by the electron liquid in the formation of the equilibrium condition of a metal, and is actually connected with the fact that the Cauchy relations are not satisfied for a homogeneous electron gas. It corresponds to a term in (6.7), which can be rewritten also in the form

$$(c_{12}-c_{44})_0=\int_0^{n_0}dn_0 n_0^2\frac{\partial}{\partial n_0^2}\frac{1}{\pi(0)}=-2P^{(0)}+\frac{1}{\varkappa^{(0)}}. \tag{6.8}$$

It is interesting that this contribution does not reduce merely to double the pressure of the electron liquid, as was sometimes assumed in the earlier papers.

Expression (6.8) depends only on the properties of the electron liquid and can be obtained for concrete metals if one uses the energy $E^{(0)}$, for example in the Nozieres-Pines interpolation form[4]. By way of example, we present here the values of this quantity for Na, K, and Al:

$$\text{Na } (c_{12}-c_{44})_0 = 0.176, \quad \text{K } (c_{12}-c_{44})_0 = 0.096,$$
$$\text{Al } (c_{12}-c_{44})_0 = 0.250.$$

The experimental values of the elastic moduli yield 0.092, 0.059, and 1.176, respectively, for this difference. Thus, the nonpaired character of the indirect inter-ion interaction turns out to be appreciable here even in the case of alkali metal, and is decisive in the case of aluminum.

7. EQUATION OF STATE OF A METAL. THE "ZERO MODEL"

The expressions (6.3) (or (6.6)) obtained in the preceding chapter is actually the equation of state of the metal for the given structure at T = 0:

$$P = P(\Omega_0). \tag{7.1}$$

The equilibrium condition in the absence of external pressure

$$P(\Omega_0) = 0 \tag{7.2}$$

enables us, knowing the pseudopotential, to find the equilibrium volume of the unit cell. Since the equilibrium value $\Omega_0(0)$ is usually known from experiment with high accuracy, Eq. (7.2) can be effectively used as an independent relation between the parameters if the effective electron interaction is specified by way of a model.

As shown by a direct analysis, in simple nontransition metals the contribution of $P^{(2)}$ is relatively small, and for a semi-quantitative analysis it is very convenient to use the so-called "zero model"[40,41], in which the structurally-dependent electronic terms are omitted. The equation of state in this model is the simple form

$$P = P^{(0)} + \frac{bz}{\Omega_0^2} - \frac{1}{3}\gamma\frac{z^2e^2}{\Omega_0^{4/3}}, \tag{7.3}$$

where γ is a constant that enters in the expression for the energy of the ion lattice (per ion)

$$E_i = -\gamma\frac{z^2e^2}{\Omega_0^{1/3}},$$

and is directly connected with the Madelung constant. The zero model is particularly effective in the case of metals of the Na or K type, where the Fourier components of the pseudopotential are small at the reciprocal-lattice points.

For the compression modulus we have accordingly in the "zero model"

$$B = \frac{z^2}{\Omega_0^2\pi(0)} + \frac{2bz}{\Omega_0^3} - \frac{4}{9}\gamma\frac{z^2e^2}{\Omega^{4/3}}. \tag{7.4}$$

From the form of expressions (7.3) and (7.4) and from the direct estimate of the terms that are contained in them it follows that a very important role is played in nontransition metals, under equilibrium conditions, by the non-Coulomb part of the averged electron-ion interaction, i.e., by the second terms of (7.3) and (7.4). The equilibrium volume is primarily the result of competition between this contribution and the contribution determined by the energy of the ion lattice.

In the model of pointlike ions, i.e., at b = 0, the pressure and the compressibility at ordinary densities turns out to be in general negative. This makes it possible, in particular, to understand why a stable metallic phase of hydrogen should correspond to a much higher density in comparison with alkali metals (the competition between the contributions from E_i and $E^{(0)}$)[30].

In the case of metals of the Na or K type, the contribution from $E^{(0)}$ is also small. Equations (7.3) and (7.4) therefore lead directly to a universal law for the equation of state[40,41]

$$\frac{P}{B(0)} = \frac{3}{2}\left[\left(\frac{\Omega_0(0)}{\Omega_0}\right)^2 - \left(\frac{\Omega_0(0)}{\Omega_0}\right)^{4/3}\right] = f\left(\frac{\Omega_0}{\Omega_0(0)}\right) \tag{7.5}$$

($B_0(0)$ and $\Omega_0(0)$ are the bulk modulus and the volume of the unit cell at P = 0). It is interesting that this law was empirically established in the analysis of the experimental data for alkali metals[42].

Figure 5 shows the equation of state obtained in[40] in terms of these variables, and the corresponding experimental points for Na and K from[26,43]. We see that there is good agreement in a relatively wide range of pressures.

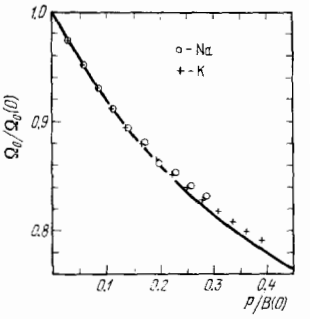

FIG. 5. Equations of state for Na and K.

8. SINGULARITIES OF ELECTRONIC MANY-POINT DIAGRAMS

It is clear from the preceding chapters that in multielectron theory an important role is played by many-point diagrams $\Gamma^{(n)}$, or diagrams with an arbitrary number of external-field lines, in which all the properties of the electronic Fermi liquid are contained. To analyze particular problems, it is necessary to have for them explicit analytic representations (see Chap. 11 below). However, in many cases (singularities in the phonon dispersion law, asymptotic behavior of the inter-ion interaction, etc.), greatest interest attaches only to the "singular" part of these many-point diagrams, i.e., to the character and the position of the singularities of the many-point diagrams as functions of the external momentum. We start with a general analysis of just this problem.

The authors have previously[44] developed a method that makes it possible to find the singularities of the many-point diagrams without an explicit analytic calculation of the diagrams. This method is in a certain sense an analog of the Landau method[45] for the determination of the singularities of diagrams in quantum field theory. The main peculiarity that distinguishes essentially the case of electronic many-point diagrams is due to the presence of a background of Fermi particles and of the Fermi surface in momentum space, and also to the three-dimensional character of the problem, all these factors taken together lead to singularities of the distinct type.

We consider in detail ring diagrams, i.e., diagrams that do not contain electron-electron interaction lines (Fig. 6).

As will be made clear later on, it is precisely these diagrams which determine the leading singularities of the many-point diagram, i.e., of the entire aggregate of diagrams with a fixed number of external-field ends.

To take the influence of the distortion of the Fermi surface into account in many-point diagrams of high order (with $n \geq 4$) (see Chap. 2), we shall use a temperature technique[23] and then let $T \to 0$. A characteristic feature of ring diagrams with static external ends, which are the only ones involved in the preceding chapters (by virtue of the adiabaticity of the problem), is the

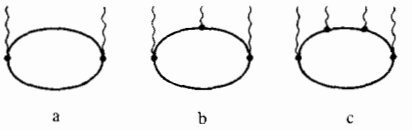

FIG. 6

presence of one and the same frequency ω in all the electronic propagators. It can be easily seen that taking the limit as $T \to 0$ is equivalent to the use of the following representation for the Green's function of the free electrons:

$$G_0(\mathbf{p}, \omega) = \frac{1}{\omega - \varepsilon_0(\mathbf{p}) + i\delta \operatorname{sgn}(\omega - \mu)}, \tag{8.1}$$

where $\epsilon_0(\mathbf{p}) = \mathbf{p}^2/2m$ and μ is the chemical potential. As $\delta \to 0$, this expression coincides with the usual one[23], but has for our purposes the advantage that the imaginary increment in the denominator of (8.1) is the same for all the Green's functions of the ring. A ring diagram with n external-field ends (see Fig. 6c) corresponds to the following expression (we omit the coefficients whose inclusion causes this expression to coincide with $\Gamma^{(n)}(\mathbf{q}_1, \ldots, \mathbf{q}_n)$):

$$I^{(n)}(\mathbf{q}_1, \ldots, \mathbf{q}_n) = \\ = \frac{2}{i} \int \frac{d\mathbf{p}\, d\omega}{(2\pi)^4} \frac{1}{[\omega - \varepsilon_0(\mathbf{p}_1) + i\delta \operatorname{sgn}(\omega - \mu)] \ldots [\omega - \varepsilon_0(\mathbf{p}_n) + i\delta \operatorname{sgn}(\omega - \mu)]}; \tag{8.2}$$

here all the $\mathbf{p}_i$ are linearly connected with $\mathbf{p}$ and $\mathbf{q}_i$. Using the well known Feynman parametrization formula, we can rewrite (8.2) in the form

$$I^{(n)}(q_1, \ldots, q_n) = (n-1)! \frac{2}{i} \int \frac{d\mathbf{p}\, d\omega}{(2\pi)^4} \int_0^1 \int_0^1 \frac{d\alpha_1 \ldots d\alpha_n}{[f]^n} \delta\Big(\sum_{i=1}^n \alpha_i - 1\Big), \tag{8.3}$$

$$f = \omega - \sum_{i=1}^n \alpha_i \varepsilon_0(\mathbf{p}_i) + i\delta \operatorname{sgn}(\omega - \mu). \tag{8.4}$$

In (8.4) we have used in explicit form the condition

$$\sum_{i=1}^n \alpha_i = 1. \tag{8.5}$$

According to the "Hadamard principle" a singularity of a multiple integral of the type (8.3) appears only if the aggregate of the real parameter $\mathbf{q}_i^{(0)}$ is such that f vanishes, and furthermore at a point where simultaneously each integration variable corresponds to: 1) a second-order zero or (2) coincidence with fixed boundaries of the integration contour. Let us analyze expressions (8.3) and (8.4) from this point of view.

From the form of (8.4) it follows directly that in ω the singularity can be only of the second type. In the integration with respect to ω, the entire integration contour can be shifted, with the exception of the point $\omega = \mu$, which remains fixed. We then obtain the first condition

$$\omega = \mu. \tag{8.6}$$

The singularity with respect to the variable $\mathbf{p}$, to the contrary, can only be of the first type. The condition $\partial f/\partial \mathbf{p} = 0$ leads in this case to the relation

$$\sum_{i=1}^n \alpha_i \mathbf{p}_i = 0. \tag{8.7}$$

The singularity with respect to the variables α_i can be of either the first or the second type. In the former case, after first eliminating α_n from (8.3) with the aid of (8.5), we obtain from the condition $\partial f/\partial \alpha_i = 0$

$$\varepsilon_0(\mathbf{p}_i) = \varepsilon_0(\mathbf{p}_n).$$

Taking into account the alternative possibility of the occurrence of a boundary singularity with respect to any of the variables α_i, and also the condition f = 0, we ultimately obtain

$$\varepsilon_0(\mathbf{p}_i) = \mu \text{ or } \alpha_i = 0 \quad (i = 1, 2, \ldots, n). \tag{8.8}$$

Thus, the necessary condition for the appearance of a singularity in the function $\Gamma^{(n)}(\mathbf{q}_1, \ldots, \mathbf{q}_n)$ (8.2) is satisfaction of the relations (8.7) and (8.8). If $\alpha_i = 0$ the propagator corresponding to a given electron line drops out in general, and the singularity corresponds to the singularity of a diagram of lower order ("reduced" diagram) obtained by contracting the given electron line to a point.

We now determine the character of the resultant singularities. To this end we carry out in (8.3) integration with respect to ω and then with respect to $\mathbf{p}$ in explicit form. Direct calculation yields

$$I^{(n)}(\mathbf{q}_1, \ldots, \mathbf{q}_n) = \frac{m}{\pi^2}(-1)^{n-1} \frac{\partial^{n-2}}{\partial \mu^{(n-2)}} \int_0^1 d\alpha_1 \int_0^{1-\alpha_1} d\alpha_2 \ldots \int_0^{1-\alpha_1-\ldots-\alpha_{n-2}} d\alpha_{n-1} \\ \times \Big/ 2m\mu + \sum_{i,j=1}^{n-1} (\varkappa_i \varkappa_j)\alpha_i \alpha_j - \sum_{i=1}^{n-1} \alpha_i \varkappa_i^2; \tag{8.9}$$

here

$$\varkappa_s = \mathbf{q}_1 + \ldots + \mathbf{q}_s. \tag{8.10}$$

It is assumed in (8.9) that the integration is carried out only over regions where the radicand is positive. In addition, we have taken into account the fact that $\varkappa_n = 0$ and integrated explicitly with respect to α_n.

The quadratic form under the square root in (8.9) is positive-definite, since it is made up of coefficients constituting a Gram determinant. At a fixed value of the external momenta $\mathbf{q}_i$, the radicand has a minimum at the point $\{\bar{\alpha}_i\}$, which is the solution of the system of equations

$$\sum_{j=1}^{n-1} (\varkappa_i \varkappa_j)\bar{\alpha}_j = \frac{1}{2}\varkappa_i^2. \tag{8.11}$$

At this point, the expression under the square root becomes equal to (K_F is the Fermi momentum)

$$\Delta = K_F^2 - \varkappa^2, \quad \varkappa^2 = \Big(\sum_{i=1}^{n-1} \bar{\alpha}_i \varkappa_i\Big)^2. \tag{8.12}$$

We note that the conditions for the existence of the singularity (8.7) and (8.8) leads, naturally, to the same system of equations (8.11), and at the singularity point itself we have

$$\Delta = 0. \tag{8.12'}$$

The singularity is realized here only at those external-momentum values $\mathbf{q}_i^{(0)}$ (or $\varkappa_i^{(0)}$) for which the solution of the system (8.11), corresponding to (8.12), lies in the integration region of (8.9).

Expanding the radicand of (8.9) at small values of Δ near $\{\alpha_i^{(0)}\}$, and carrying out the integration for the singular part of $I^{(n)}$, we obtain after a number of transformations[44]

$$I_{\text{sing}}^{(n)} \sim (-1)^{(2n+s-1)/2} \frac{\partial^{(n-2)}}{\partial \Delta^{(n-2)}} (\Delta^{(s+1)/2} \ln|\Delta|) \sim \\ \sim (-1)^{(2n+s-1)/2} \Delta^{(s-2n+5)/2} \ln|\Delta| \quad (\text{s is odd}), \tag{8.13}$$

where Δ can be of arbitrary sign;

$$I_{\text{sing}}^{(n)} \sim (-1)^{(2n+s+2)/2} \frac{\partial^{(n-2)}}{\partial \Delta^{(n-2)}} \Delta^{(s+1)/2} \sim \\ \sim (-1)^{(2n+s+2)/2} (\Delta)^{(s-2n+5)/2} \quad (\text{s is even}, \Delta > 0); \tag{8.14}$$

at $\Delta < 0$, the diagram has no singularities. Here s is the rank of the square matrix made up of $\varkappa_i$:

$$\|\varkappa_i \varkappa_k\|. \tag{8.15}$$

Expressions (8.13) and (8.14) determine the behavior of

$I^{(n)}$ near a leading singularity of a ring diagram with n ends. Such a diagram contains in fact also weaker "boundary" singularities, corresponding to the vanishing in (8.8) of one or several α_i. The behavior of $I^{(n)}$ near the boundary singularity corresponding to k values $\alpha_i = 0$ is described by the same expressions (8.13) and (8.14), with the substitutions

$$n \to n' = n - k, \quad s \to s',$$

where s' is the rank of the square matrix of order n' remaining after crossing out k rows and columns, with the indices corresponding to $\alpha_i = 0$, from the initial matrix $\|\kappa_i \kappa_k\|_k$.

Expressions (8.13)–(8.14) together with (8.6)–(8.8) (or (8.11)–(8.12)) solve completely the problem of the character and position of the singularities of the ring diagrams with tails of a static external field for the system of Fermi particles. At the same time, it seems that these singularities remain leading also for the entire many-point diagram with n external-field ends. Indeed, the most remarkable result is the fact that in order for singularities to appear it is necessary that all the virtual particles lie on the Fermi surface (see (8.8)). This is a reflection of the role played by the sharp boundary in momentum space, which is typical of the Fermi distribution. When account is taken of the interaction between the electrons this sharp boundary, as is well known, is preserved (see[46], and also[23]). On the other hand, each interaction line is accompanied on the more complicated diagrams by two electronic propagators and simultaneously by additional quadrupole integration. It can be assumed as a result that allowance for the diagrams with inter-electron interaction leads to neither the appearance of stronger singularities nor to a smearing of the singularities obtained above.

We consider now the singularities of separare particular many-point diagrams. In the case of a two-point diagram (see Fig. 6a), the solution of (8.11) yields $\bar{\alpha}_i = 1/2$. Then, recognizing that s = 1 and $\kappa_1 = q_1$, we obtain from (8.12) and (8.13) for the singular part

$$I^{(2)}_{\text{sing}}(\mathbf{q}_1, -\mathbf{q}_1) \sim \left(K_F^2 - \frac{q_1^2}{4}\right) \ln\left(K_F^2 - \frac{q_1^2}{4}\right). \qquad (8.16)$$

We arrive at the known singularity typical of the usual polarization loop[47].

For a three-point diagram (see Fig. 6b), the rank of the matrix (8.15) is s = 2, and the solution of the system yields

$$\bar{\alpha}_1 = \frac{1}{2}\varkappa_2^2 \frac{\varkappa_1^2 - \varkappa_1\varkappa_2}{\varkappa_1^2\varkappa_2^2 - (\varkappa_1\varkappa_2)^2}, \quad \bar{\alpha}_{22} = \frac{1}{2}\varkappa_1^2 \frac{\varkappa_2^2 - \varkappa_1\varkappa_2}{\varkappa_1^2\varkappa_2^2 - (\varkappa_1\varkappa_2)^2}.$$

The sum of these quantities should be less than one. This leads immediately to the limitation

$$\widehat{\varkappa_1, \varkappa_2} < \frac{\pi}{2}.$$

Taking into account (8.10) ($\kappa_1 = q_1$, $\kappa_2 = -q_3$) and the leeway in the numbering of the external momenta, we can conclude from this condition that the singularity exists only if the vectors q_1, q_2, and q_3 form an acute triangle.

Using the obtained values of $\bar{\alpha}_i$ from (8.12), we get

$$\varkappa^2 = \frac{1}{4}\frac{(\varkappa_1 - \varkappa_2)^2}{1 - [(\varkappa_1\varkappa_2)^2/\varkappa_1^2\varkappa_2^2]} = \frac{1}{4}\frac{q_3^2}{\sin^2(\widehat{q_1 q_3})} = q_R^2,$$

where q_R is the radius of the circumscribed circle of the triangle made up of the vectors q_1, q_2, and q_3. We then obtain from (8.14) for the singular part of the three-point diagram

$$I^{(3)}_{\text{sing}}(\mathbf{q}_1, \mathbf{q}_2, \mathbf{q}_3) \sim \sqrt{K_F^2 - q_R^2}, \quad q_R < K_F. \qquad (8.17)$$

($I^{(3)}$ is an analytic function at $q_R > K_F$.) In the degenerate case when the vectors q_1 and q_2 are parallel, the rank of the matrix (8.15) decreases to s = 1, and we arrive at the stronger singularity

$$I^{(3)}_{\text{sing}}(\mathbf{q}_1, -\mathbf{q}_1, 0) \sim \ln\left|K_F^2 - \frac{q_1^2}{4}\right|. \qquad (8.18)$$

In the case of a four-point diagram we obtain for the leading singularity (s = 3) from (8.13)

$$I^{(4)}_{\text{sing}}(\mathbf{q}_1, \mathbf{q}_2, \mathbf{q}_3, \mathbf{q}_4) \sim \ln|K_F^2 - \varkappa_R^2|, \qquad (8.19)$$

where κ_R^2 is obtained from (8.11) and (8.12) and corresponds to the radius of the sphere circumscribed around a tetrahedron with sides q_1, q_2, q_3, q_4, $q_1 + q_2$, and $q_1 + q_3$. If all the vectors lie in one plane, then the rank of the matrix decreases to s = 2 and we have in this case from (8.14)

$$I^{(4)}_{\text{sing}}(\mathbf{q}_1, \mathbf{q}_2, \mathbf{q}_3, \mathbf{q}_4) \sim \frac{1}{\sqrt{K_F^2 - \varkappa^2}}, \quad \varkappa < K_F. \qquad (8.20)$$

For many-point diagrams of higher order, we arrive at an interesting problem connected with the fact that space is three-dimensional, i.e., with the fact that $s \leq 3$ always, and the number of external ends increases. We shall not analyze this case here, referring the reader to the cited paper[44] for details.

All the singularities considered above become clearly manifest on the dispersion curves of phonons in metals. This question is considered in greater detail in the next chapter.

9. ANOMALIES ON THE PHONON DISPERSION CURVES

As shown in the preceding chapter, the presence of a sharp Fermi boundary in the momentum distribution of the electrons leads to the appearance of an entire "hierarchy" of singularities in the electronic many-point diagrams (8.13)–(8.14).

An essential fact is that singularities of this kind can be observed in experiment directly, by measuring the phonon dispersion curves. Indeed, in the study of phonons in the entire momentum space, a continuous variation of q leads inevitably to satisfaction of the critical conditions (8.9) for the many-point diagrams that enter in the dynamical matrix (3.12). The simplest of the considered singularities is the two-point-diagram singularity corresponding to the polarization operator of a homogeneous electron gas. The first statement that this singularity should become manifest in the phonon spectrum was made by Kohn[48]. The "Kohn" singularity was subsequently observed many times in experiments on inelastic neutron scattering ([49-51] etc.). From the form of the dynamic matrix it follows that the singularity for a phonon with wave vector q occurs under the condition

$$|\mathbf{q} + \mathbf{K}| = 2K_F. \qquad (9.1)$$

If the Fermi surface becomes strongly restructured near the boundaries of the Fermi zone, then singularities at certain other values of q can appear in principle, in addition to the singularities of the points (9.1), which can be shifted somewhat. This can be easily understood by using the analysis of Chap. 8. Indeed, when explicit account is taken of the anisotropy of the electron dis-

persion law in the Green's functions, the condition (8.7) is replaced by

$$\sum \alpha_i \frac{\partial \varepsilon(\mathbf{p}_i)}{\partial \mathbf{p}_i} = \sum_i \alpha_i \mathbf{v}_i(\mathbf{p}_i) = 0; \qquad (9.2)$$

here $\mathbf{v}_i(\mathbf{p})$ is the group velocity of the electrons. (The remaining conditions remain unchanged.) From the condition that α_i be positive it follows immediately in the case of a two-point diagram that the singularity takes place for the vectors $\mathbf{q} + \mathbf{K}$ joining two Fermi-surface points that have strictly oppositely directed group velocities. In the case of a spherical Fermi surface, the condition (9.2) coincides with (9.1), but additional singularities can appear in the case of strong distortion. In this case the character of the singularities can be greatly strengthened; for example, for pieces of the Fermi surface of cylindrical form, the singularity of the derivative becomes of the root type, and for flat pieces of the surface the singular part itself becomes logarithmic[52]. It is interesting that the "flat" situation takes place for electrons in a strong magnetic field[53].

The singularities corresponding to more complicated diagrams ($\Gamma^{(n)}$) are connected with the indirect interaction between three and more ions, and the corresponding many-point diagrams enter in the dynamical matrix with several momenta equal to the reciprocal-lattice vectors. Let us consider in greater detail the singularity corresponding to the three-point diagram. In this case, as seen from (3.12), one of the momenta, say $\mathbf{q}_3$, should be equal to the reciprocal-lattice vector $\mathbf{K}_3$. From the previously obtained condition it is therefore clear that the "triangular" singularities can be produced only by vectors $|\mathbf{K}| < 2|\mathbf{K}_f|$. Consequently, neither these singularities nor more complicated ones appear at all in monovalent metals. Singularities occur only in polyvalent metals and only for the reciprocal-lattice vectors with the smallest moduli. It is necessary here to satisfy the condition $q_R = K_F$ in a triangle with sides $\mathbf{q} + \mathbf{K}_1$, $\mathbf{q} - \mathbf{K}_1 - \mathbf{K}_3$, and $\mathbf{K}_3$.

Figure 7 shows a geometric construction that demonstrates the position and the character of the singularity in a metal with bcc structure and $r_s \sim 2$ (the characteristic density of Pb). The "Kohn" anomalies corresponding to diagrams that are reduced from the "three-point diagram" are also indicated, and are connected with both $\mathbf{q}_1$ and $\mathbf{q}_2$. We chose a definite reciprocal-lattice vector corresponding to the site [111] and considered several phonon propagation directions q (labeled by the numbers). Singularities occur when the end of the vector q, designated O_3, crosses a circle of radius K_F drawn on the vector [111]. The figure shows clearly how the singularity, which is strongly pronounced for acute triangles (2, 3, 4), becomes smoothed out and vanishes for obtuse triangles, for example (6). This circumstance can be used for an experimental separation of triangular singularities from "Kohn" singularities.

It should be noted that the results obtained in Chap. 8 correspond to the use of perturbation theory in the electron-ion interaction, and cannot be used for electrons near Brillouin planes. Inasmuch as one of the vectors of the three-point diagram should be equal to the reciprocal-lattice vector, expression (8.17) holds outside a narrow region near the singularity. Inside this region, on the other hand, the behavior of the three-point diagram has a more complicated character that depends on the particular form of the Fermi surface and of the wave

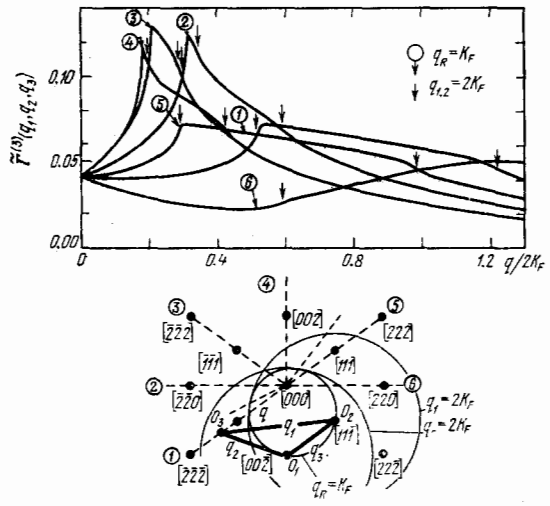

FIG. 7. Geometry and general form of the singularity of a "three-point diagram" for different angles of the triangle.

functions of the electron, and the singularity becomes smeared out. This is a general result for the appearance of singularities of many-point diagrams on phonon dispersion curves. The only exception is the singularity of a two-point diagram, which does not become smeared out. However, as seen from Fig. 7, the anomalous character of the three-point diagram takes place in a much broader region. Therefore, in spite of the smearing, it can become manifest to a sufficiently strong degree. It should be noted that although many-point diagrams of higher order have stronger singularities (which also become smeared out in principle), the fact that an additional factor V_K/ϵ_F appears each time with increasing n makes the separation of the singularities of many-point diagrams with $n > 3$ difficult.

The appearance of singularities on dispersion curves that reflect the topology of the Fermi surface is one of the clearest manifestations of the role of electrons in the formation of the phonon spectrum. Unlike nonmetals, where $\omega_\alpha(\mathbf{q})$ is an analytic function of q, in any case outside the degeneracy points, this function is clearly nonanalytic in a metal.

Singularities in the phonon spectrum correspond to infinite values of the group velocity $v_\alpha(\mathbf{q}) = \partial\omega_\alpha(\mathbf{q})/\partial\mathbf{q}$. They should therefore be most clearly pronounced precisely on plots of the group velocity against q. Figures 8 and 9 show theoretical plots of $v_\alpha(\mathbf{q})$ for three symmetrical directions in the case of Na and Al, obtained with the terms $E^{(2)}$ and $E^{(3)}$ taken into account. We see how strikingly different the curves are: there is practically no fine structure in the former case and an exceptionally strongly pronounced fine structure in the latter.

The result for Na can be easily understood if account is taken of the smallness of the ratio $V_{|\mathbf{q}|=2K_F}/\epsilon_F$, which is typical of alkali metals, and if it is recognized that $|\mathbf{K}_{min}| > 2K_F$ in such metals, and consequently there are no singularities for three-point diagrams (and for many-point diagrams of higher order in general). The picture is particularly remarkable because it is difficult to guess, by simply glancing at the dispersion curves of the two metals (see below), how different is the information that they contain. In particular, it becomes clear why it is so easy to describe the Na spectrum within the framework of the phenomenological model of

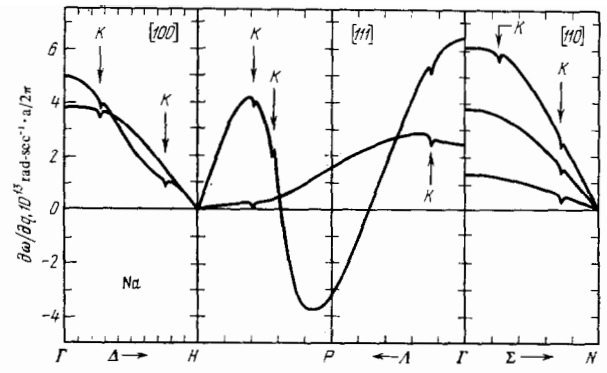

FIG. 8. Group velocity $\partial\omega/\partial q$ for phonons in Na.

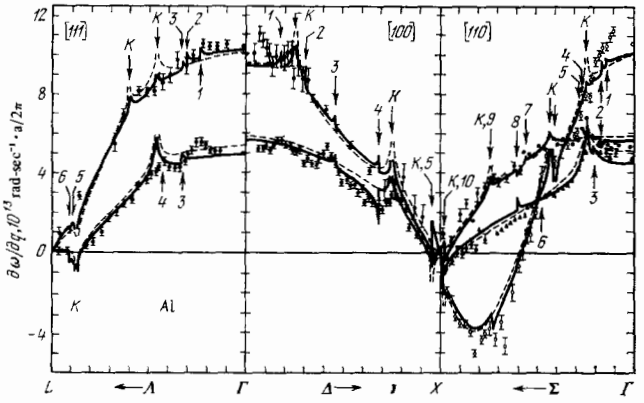

FIG. 9. Group velocity $\partial\omega/\partial q$ for phonons in Al.

short-range forces, in contrast to metals such as aluminum.

The curves in Fig. 9 are quite unique in form. The regions of smooth variation of $v_\alpha(\mathbf{q})$ are separated by numerous singularities of either the "Kohn" or three-point-diagram type. The "Kohn" type singularities are only of the "diametral" type, i.e., they are connected with the initial sphere of the quasifree electrons and by the same token with the condition (9.1). We have already noted that the phonon-spectrum singularities connected with allowance for many-ion interaction are not true mathematical singularities and should become partly smeared out. Consequently the behavior of the curves near the singularities of the three-point diagram are drawn arbitrarily. It is interesting that although each singularity connected with non-paired interaction contains an extra factor V_K/ϵ_F, a strong restructuring of entire regions of the curves takes place as a result of the strong character and considerable interval of the singularity.

Figure 9 shows also the results of exceptionally precise measurements by Weymouth and Stedman[54], which enabled them to determine the group velocity of the phonons in aluminum as a function of q. Their study was devoted specially to searches for Kohn anomalies. In addition to these two-point-diagram anomalies, which appear on the theoretical curve, the authors obtained many anomalies due to restructuring of the electron spectrum near the Brillouin-zone boundaries, and the positions of these anomalies are governed by the positions of the points on the Fermi surface at which the group velocities of the electrons are antiparallel (see (9.2)).

They observed at least two singularities that cannot be identified as "Kohn" singularities. They are located at q = 0.43 along the [100] direction and q = 0.33 along the [110] direction (in units of $2\pi/a$). A direct analysis has shown that the positions of these singularities coincide with the positions of the singularities of the three-point diagram (in the former case $K_1 = 0, 0, -2$, $K_2 = 1, 1, -1$, $K_3 = 1, 1$, and there are 16 equivalent sets of reciprocal-lattice vectors, and in the latter case $K_1 = 1, -1, -1$, $K_2 = 2, 0, 0$, and $K_3 = 1, 1, 1$ and the number of equivalent sets is eight).

Thus, singularities corresponding to three-particle interaction have apparently been observed for the first time in this experiment.

We note in conclusion the general reasonable correspondence between the theoretical curves and the experimental results, which is far from trivial at the level of the derivative of the phonon dispersion law, and can be attained in principle only within the framework of a microscopic analysis.

10. INTER-ION FORCES IN A METAL. COVALENCE

The entire preceding analysis of the static and dynamic characteristics of a metal was carried out in momentum space. In principle, however, an alternative description in coordinate space is possible. Indeed, by virtue of the validity of the adiabatic approximation, the energy of the electron system in the field of ions plays the role of a potential in the problem of ion motion (see Chap. 1). This potential (see (2.5)) can be regarded as an effective inter-ion interaction, and we thus arrive at the concept of forces binding the ions in the metal.

This concept, as already indicated, is not necessary for the problems considered here. Nonetheless, it is useful for a discussion of a number of physical questions that are traditionally considered in direct space, for example the covalence question. Traditional crystal dynamics was also formulated precisely in this language[5]. In particular, metals were regarded as characterized by the presence of a paired centrally-symmetrical interaction between ions, corresponding to additivity of the forces.

Yet the theory developed above shows that much more complicated inter-ion interactions are realized in a metal. Indeed, paired simple forces arise naturally from a direct ion-ion interaction and from an indirect interaction

$$\varphi_2^{(2)}(\mathbf{R}_1-\mathbf{R}_2)=\frac{2!\,\Omega}{N^2}\sum_{\mathbf{q}\neq 0}\Gamma^{(2)}(\mathbf{q},-\mathbf{q})\,|V_{\mathbf{q}}|^2 e^{i\mathbf{q}(\mathbf{R}_1-\mathbf{R}_2)}. \qquad (10.1)$$

However, in addition to these there are also interactions that bind groups of three and more ions. Thus, from the term $E^{(3)}$ we find ($\mathbf{R}_1 \neq \mathbf{R}_2 \neq \mathbf{R}_3$)

$$\varphi_3^{(3)}(\mathbf{R}_1-\mathbf{R}_3,\,\mathbf{R}_2-\mathbf{R}_3)=\frac{3!\,\Omega}{N^3}\sum_{\mathbf{q}_1,\,\mathbf{q}_2\neq 0}\Gamma^{(3)}(\mathbf{q}_1,\,\mathbf{q}_2,\,-\mathbf{q}_1-\mathbf{q}_2)$$
$$\times V_{\mathbf{q}_1}V_{\mathbf{q}_2}V_{-\mathbf{q}_1-\mathbf{q}_2}\exp\{i\mathbf{q}_1(\mathbf{R}_1-\mathbf{R}_3)+i\mathbf{q}_2(\mathbf{R}_2-\mathbf{R}_3)\}. \qquad (10.2)$$

The presence of such a term indicates immediately non-additivity of inter-ion interactions and the appearance of unique unpaired forces of the covalent type in a metal.

The expansion (2.5) indicates one more interesting circumstance. The n-th order term contains contributions not only from the interactions of n ions, but also from a smaller number of "different" ions, since this term takes into account the possibility of multiple scattering by one and the same separate ion. Thus, for example, $E^{(3)}$ contains also an indirect pair interaction as

the result of double scattering by one ion and single scattering by another:

$$\varphi_2^{(3)}(\mathbf{R}_1-\mathbf{R}_2) = 3\cdot 2!\,\frac{\Omega}{N^3}\sum_{\mathbf{q}_1,\,\mathbf{q}_2\neq 0} e^{i\mathbf{q}_1(\mathbf{R}_1-\mathbf{R}_2)}\,\Gamma^{(3)}(\mathbf{q}_1,\,\mathbf{q}_2,\,-\mathbf{q}_1,\,-\mathbf{q}_2)\,V_{\mathbf{q}_1}V_{\mathbf{q}_2}V_{-(\mathbf{q}_1+\mathbf{q}_2)}. \quad (10.3)$$

In addition, there is also a homogeneous term due to the triple scattering by an individual ion:

$$\varphi_1^{(3)} = \frac{\Omega}{N^3}\sum_{\mathbf{q}_1,\,\mathbf{q}_2\neq 0}\Gamma^{(3)}(\mathbf{q}_1,\,\mathbf{q}_2,\,-\mathbf{q}_1-\mathbf{q}_2)\,V_{\mathbf{q}_1},\,V_{\mathbf{q}_2}V_{-(\mathbf{q}_1+\mathbf{q}_2)}. \quad (10.4)$$

A similar term is contained, obviously, also in $E^{(2)}$:

$$\varphi_1^{(2)} = \frac{\Omega}{N}\sum_{\mathbf{q}}\Gamma^{(2)}(\mathbf{q},\,-\mathbf{q})\,|V_{\mathbf{q}}|^2. \quad (10.5)$$

It is clear that in the general case the electron energy can be represented in the form of the series

$$E_e = \varphi_0 + \sum_n \varphi_1(\mathbf{R}_n) + \frac{1}{2!}\sum_{n\neq m}\varphi_2(\mathbf{R}_n-\mathbf{R}_m) + \frac{1}{3!}\sum_{n\neq m\neq l}\varphi_3(\mathbf{R}_n-\mathbf{R}_m,\,\mathbf{R}_n-\mathbf{R}_l). \quad (10.6)$$

Each term of this expansion, which describes simultaneous indirect interaction between k different ions, can in turn, in accord with the foregoing, be represented in the form of the series

$$\varphi_k(\{\mathbf{R}_l\}) = \sum_{p\geq k}\varphi_k^{(p)}(\{\mathbf{R}_i\}) \quad (10.7)$$

If we analyze the obtained expressions, we come across the following interesting result. The series (10.6) and (10.7) are expansions in powers of the electron-ion interaction, but by no means in powers of the small parameter V_K/ϵ_F, as, for example, in (2.16). From each term of definite order in V_K/ϵ_F, for example from $E^{(3)}$, we obtain several terms (10.2)—(10.4) containing V_q already in the intermediate momentum regions, where the potential, generally speaking, is not weak (see (3.13)). If the role of the small $\mathbf{q}$ in (10.3) and (10.4) is appreciable, as is the case in a number of polyvalent metals, then the convergence of the series (10.7) turns out to be slow. In particular, pair interaction, which in accordance with the usual practice is taken only from $E^{(2)}$, is in fact appreciably altered, and this may turn out to be important for many problems that use coordinate representations, for example for the description of vacancies. It would therefore be attractive to construct a technique for the summation of the series (10.7) and to express the answer, for example, in terms of an exact amplitude for the scattering of an electron by an individual ion. However, owing to the presence of electron-electron interaction at the typical metallic electron densities, this is strictly speaking impossible.

We note that this is not necessary for our problem, since interference produces in a metallic equilibrium crystal, as a whole, a mutual cancellation of the electron scattering corresponding to the terms $\varphi_K^{(p)}$ at a fixed value of p. As a result, the only remaining contributions are those from electron scattering with transfer of a momentum equal to the reciprocal-lattice vectors. This is precisely why the total inter-ion interaction in a metal is expressed in the form of a series in powers of the small parameter V_K/ϵ_F, although the interactions themselves, in clusters consisting of several ions in the electron fluid, do not contain this parameter in explicit form, and the series (10.7) as described by expansions that converge more slowly. Consequently, the separation of paired and non-paired interactions from the terms of definite order in V_K/ϵ_F in (2.5) is much less effective in the calculations than the determination of their joint contribution. Thus, for example, the corrections to the pair interaction from $E^{(3)}$ (10.3) are of the same order as the three-particle interaction (10.2) from the same term, as can be shown by a direct analysis (see[28]), and as a rule are larger than $E^{(3)}$ itself.

Thus, the cooperative character of the interactions in the metal leads to the onset of complicated unpaired forces, which represent forces that unify clusters of three, four, etc. ions. If for some reason phase-space regions near the boundaries of Brillouin zones become significant, then to describe the contributions of such a region to the interaction we must use expressions of the type (3.16), without expanding in the electron potential. This gives rise to one more increment to (10.6), which has no "cluster" character, but pertains in coherent fashion to the entire crystal as a whole. Such non-paired terms, in particular, should be significant for the coupling and dynamics of oscillations of semiconductors, where there is no free Fermi surface at all, and also in those metals having a large number of gaps that "fall" on the Fermi surface (e.g., in Be). For most metallic crystals (and also liquid metals) they do not seem to play a noticeable role.

Let us discuss the asymptotic behavior of the resultant forces. The total indirect pair interaction between ions is described by the term φ_2 in (10.6). The first term of the expansion (10.7) for φ_2 is the usual expression used to describe the interaction between two ions in an electron liquid (see, e.g.,[1]), which leads to an axially-symmetrical force matrix in the form (3.7). As is well known, since the polarization operator is not analytic at $|\mathbf{q}| = 2K_F$ (see (8.16)), the function $\varphi_2^{(2)}$ (10.1) has a non-exponential asymptotic form (Friedel oscillations)

$$\varphi_2^{(2)} \sim \frac{\cos 2K_F|\mathbf{R}_1-\mathbf{R}_2|}{K_F^3|\mathbf{R}_1-\mathbf{R}_2|^3}. \quad (10.8)$$

It is easy to understand that the next terms in φ_2 decrease at any rate no slower than (10.8). This can be seen from the fact that although, for example, $\Gamma^{(3)}$ has a stronger non-analyticity than $\Gamma^{(2)}$ (see (8.17)), $\Gamma_2^{(3)}$ (10.3) contains on the other hand an extra integration with respect to $\mathbf{q}$. A similar situation obtains also for all the remaining contributions to the pair interaction. Thus, the asymptotic form of the pair interaction retains the form (10.8), and the coefficient of this term is obtained as an expansion in the pseudopotential.

The long-range character of this interaction causes a slow decrease of the force-matrix parameters with the number of the coordination sphere, as first revealed by the now classical experiments on the measurement of the phonon spectrum of lead[50], where the indirect interaction plays a very important role.

We note that allowance for the nonsphericity of the real Fermi surface can change in some cases the asymptotic form of the pair forces. Thus, in the case of a strictly cylindrical Fermi surface, owing to the stronger character of the singularity ([52], see Chap. 9) we get $1/r^2$ in place of $1/r^3$, and in the case of a flat surface we even get $1/r$.

The aggregate of the terms φ_k with $k \geq 3$ describes unpaired indirect interaction at a fixed density. Comparing again the character of the leading singularity for an n-th order many-point diagram and the general expres-

sion (2.12) with the number of integrations with respect to $\mathbf{q}$, we can conclude that the unpaired interaction decreases asymptotically with increasing distance between any of the ion pairs, at a rate that is likewise not slower than (10.8).

We note in conclusion that the unpaired interaction that depends on the mutual position in space of several ions and leads to the appearance of covalent-type forces is sensitive to the structure of the crystal. It therefore differs in principle from the paired forces and cannot be imitated by any special choice of the electron-ion interaction, including also in nonlocal form. The role of the unpaired forces in the dynamics of polyvalent metals can be quite significant, and in many cases decisive, for example, in the problem of the dynamic stability of complicated metals[15,16]. All the features of this interaction are manifest already in principle in the leading term (10.2), and in the dynamic matrix by the associated contribution with n = 3 (3.12). Therefore in the analysis of the phonon spectrum of polyvalent metals it is of fundamental importance to take into account at least this term in the dynamical matrix.

From the experimental point of view, particular interest attaches to a direct observation of the manifestation of unpaired forces. One possibility of such observation was already encountered by us—we have in mind the "triangular" or singularities of higher order on the phonon dispersion curves (see Chap. 9). We shall discuss here one more direct manifestation of unpaired forces, namely the lifting of the degeneracy in a phonon spectrum by these forces[55].

As already noted, paired interaction leads to axial symmetry of the force matrix for each pair of ions. As a result, the dynamic matrix can have in the general case a higher symmetry than dictated by the spatial symmetry group of the lattice. This circumstance can lead to additional symmetry in the phonon spectrum at definite points of phase space, which, however, is lifted in the presence of unpaired forces. Therefore the qualitative restructuring of the spectrum and its scale is therefore evidence of the existence of non-paired forces and of their quantitative characteristic.

A clear-cut example of this situation is the behavior of the phonon dispersion in hexagonal metals in the symmetrical point K[55]. In the absence of non-paired forces, there are two degenerate frequencies at this point, $\omega_1^2 = \omega_3^2$, and two other frequencies, ω_2^2 and ω_4^2, which are shifted away from them upward and downward by strictly equal distances. In the presence of non-paired forces, the degenerate level shifts relative to the center $(\omega_2^2 + \omega_4^2)/2$. The available experimental data on the measurement of the phonon spectrum in hexagonal metals demonstrates clearly the shift of the degenerate frequency (see, e.g., the spectrum of Mg in Fig. 13 below), and the value of this shift offers evidence of the appreciable scale of the unpaired forces. It turned out to be particularly large in Zn[56] and in Be[57].

11. CALCULATION OF IRREDUCIBLE MANY-POINT DIAGRAMS

For a quantitative analysis of the phonon spectrum in all of phase space, it is necessary to know important characteristics of the homogeneous electron liquid, namely irreducible many-point diagrams $\Lambda^{(n)}(\mathbf{q}_1, \ldots, \mathbf{q}_n)$ with arbitrary values of the momenta of the external "ends."

Of course, owing to the absence of a small parameter at the characteristic metallic densities, one cannot hope to obtain exact expressions for them. There exist at present, however, a number of interpolation schemes that make it possible to obtain sufficiently reasonable approximations (see below). In all cases it is necessary to know the principal "skeleton" structures, which serve as the basis for further approximations. It is easily understood that they correspond to many-point diagrams (for a two-point diagram—the simple polarization loop).

The representation (8.9) obtained above is very convenient for a direct integration of such ring diagrams. (A method for finding an analytic expression corresponding to an arbitrary n-point diagram was developed in[27].) For a multipoint diagram (simple loop) we obtain the well known expression[47]

$$\pi_0(\mathbf{q}) = \frac{3}{2}\frac{n}{\varepsilon_F}\left[\frac{1}{2} + \frac{1}{4}\frac{1-(q/2K_F)^2}{q/2K_F}\ln\left|\frac{1+(q/2K_F)}{1-(q/2K_F)}\right|\right]. \quad (11.1)$$

For a three-point diagram we have[44,75]

$$\Lambda_0^{(3)}(\mathbf{q}_1, \mathbf{q}_2, \mathbf{q}_3) = \frac{2}{3}\frac{m^2}{\pi^2}\frac{q_R^2}{q_1q_2q_3}\left\{\sum_m \cos\theta_m \ln\left|\frac{2K_F+q_m}{2K_F-q_m}\right|\right.$$
$$\left. -\Delta\times\begin{cases}\ln|(1-\Delta A)/(1+\Delta A)| & \text{for } K_F/q_R < 1\\ 2\operatorname{arctg}\Delta A & \text{for } K_F/q_R > 1\end{cases}\right\}; \quad (11.2)$$

here

$$\Delta = \sqrt{|(K_F/q_R)^2 - 1|},$$
$$A = \frac{q_1q_2q_3}{(2K_F)^3\{1-|(q_1^2+q_2^2+q_3^2)/2(2K_F)^2|\}}, \quad q_R = \frac{q_1q_2q_3}{2\sqrt{q_1^2q_2^2-(\mathbf{q}_1\mathbf{q}_2)^2}}, \quad (11.3)$$

q_R is the radius of the circumscribed circle, and $\cos\theta_i = -(\mathbf{q}_k\mathbf{q}_l)/q_kq_l$. The branch $0 \le \tan^{-1}x \le \pi$ is proposed for the arctangent. A similar result can be arrived at also by direct calculation of the single-electron energy in third order in the electron-ion interaction[59]. Expression (11.2) for the three-point diagram is found to be automatically symmetrical with respect to permutations of q_i.

For a four-point diagram it is necessary already to carry out a special symmetrization (the operation S):

$$\Lambda_0^{(4)}(\mathbf{q}_1, \mathbf{q}_2, \mathbf{q}_3, \mathbf{q}_4) = \frac{1}{4}SI^{(4)}(\mathbf{q}_1, \mathbf{q}_2, \mathbf{q}_3, \mathbf{q}_4); \quad (11.4)$$

the integral $I^{(4)}$ is defined in (8.9). In the general "spatial" case the formula for $I^{(4)}$ is quite cumbersome and is expressed in terms of a single integral (see[27]). If we consider the frequently encountered planar case, when all four momenta q_i lie in one plane, the integration can be carried through to conclusion, and we obtain

$$I_0^{(4)}(\mathbf{q}_1, \mathbf{q}_2, \mathbf{q}_3, \mathbf{q}_4) = 3m[P_1\Lambda^{(3)}(\mathbf{q}_1, \mathbf{q}_2, -(\mathbf{q}_1+\mathbf{q}_2))$$
$$+ P_2\Lambda^{(3)}(\mathbf{q}_2, \mathbf{q}_3, -(\mathbf{q}_2+\mathbf{q}_3)) + P_3\Lambda^{(3)}(\mathbf{q}_3, \mathbf{q}_4, -(\mathbf{q}_3+\mathbf{q}_4))$$
$$+ P_4\Lambda^{(3)}(\mathbf{q}_4, \mathbf{q}_1, -(\mathbf{q}_1+\mathbf{q}_4))]; \quad (11.5)$$

The three-point diagram $\Lambda^{(3)}$ is defined in (11.2), and

$$P_1 = \frac{2}{(\mathbf{q}_1\mathbf{q}_2)(2S_{34}^2S_{12}/4S_{12}^2+\mathbf{q}_3\mathbf{q}_4)}, \quad 2S_{34} = [\mathbf{q}_3, \mathbf{q}_4]$$

(the remaining P_i are obtained by cyclic permutation).

An important particular case of this expression is encountered when the momenta are pairwise equal:

$$\Lambda_0^{(4)}(\mathbf{q}_1, -\mathbf{q}_1, \mathbf{q}_2, -\mathbf{q}_2) = \frac{1}{12}[I_A^{(4)}(\mathbf{q}_1, \mathbf{q}_2, -\mathbf{q}_1, -\mathbf{q}_2)$$
$$+ I_B^{(4)}(\mathbf{q}_1, -\mathbf{q}_1, -\mathbf{q}_2, \mathbf{q}_2) + I_B^{(4)}(\mathbf{q}_1, -\mathbf{q}_1, \mathbf{q}_2, -\mathbf{q}_2)]; \quad (11.6)$$

here

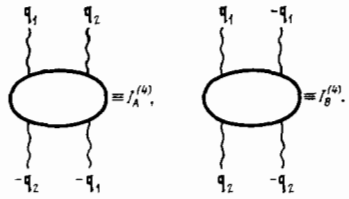

The obtained symmetrized expression for (11.6) is quite compact[27]:

$$\Lambda_0^{(4)}(\mathbf{q}_1, -\mathbf{q}_1, \mathbf{q}_2, -\mathbf{q}_2) = -\frac{m^3}{6\pi^2}\frac{(4K_F^2-q_3^{+2})}{q_1q_2q_3^+(\mathbf{q}_1\mathbf{q}_2)}\frac{1}{\Delta^+}$$
$$\times\begin{cases}-(1/2)\ln|(1-\Delta^+A^+)/(1+\Delta^+A^+)|, & K_F/q_R^+<1,\\ \operatorname{arctg}\Delta^+A^+, & K_F/q_R^+>1,\end{cases}$$
$$+\frac{m^3}{6\pi^2}\frac{(4K_F^2-q_3^{-2})}{q_1q_2q_3^-(\mathbf{q}_1\mathbf{q}_2)}\frac{1}{\Delta^-}$$
$$\times\begin{cases}-(1/2)\ln|(1-\Delta^-A^-)/(1+\Delta^-A^-)|, & K_F/q_R^-<1,\\ \operatorname{arctg}\Delta^-A^-, & K_F/q_R^->1\end{cases};$$

here $\mathbf{q}_3^{\pm} = -(\mathbf{q}_1 \pm \mathbf{q}_2)$, and the corresponding quantities $q_R^{\pm}$, $\Delta^{\pm}$, and $A^{\pm}$ have been introduced.

The diagram $I_B^{(4)}$ is of interest in that it contains an "anomalous" contribution due to the coincidence of poles from two G-functions. As already noted above, the integral representation (8.9) yields automatically the sum of the "normal" and "anomalous" contributions. However, the "anomalous" contribution can be separated in principle:

$$I_{Ba}^{(4)}(\mathbf{q}_1, \mathbf{q}_2, -\mathbf{q}_1, -\mathbf{q}_2) = -2\sum_{\mathbf{p}}\delta(\varepsilon_{\mathbf{p}}-\mu)\frac{1}{(\varepsilon_{\mathbf{p}}-\varepsilon_{\mathbf{p}+\mathbf{q}_1})(\varepsilon_{\mathbf{p}}-\varepsilon_{\mathbf{p}-\mathbf{q}_2})}. \quad (11.7)$$

The obtained integral (for the region $\mathbf{q}_1, \mathbf{q}_2 > 2\mathbf{K}_F$) can be easily calculated:

$$I_{Ba}^{(4)} = -\frac{m^3}{\pi^2}\frac{1}{q_1q_2q_3^+\Delta^+}\ln\left|\frac{q_1q_2+4K_F^2[(\mathbf{q}_1\mathbf{q}_2)/q_1q_2]+2K_Fq_3^+\Delta^+}{q_1q_2+4K_F^2[(\mathbf{q}_1\mathbf{q}_2)/q_1q_2]-2K_Fq_3^+\Delta^+}\right|. \quad (11.8)$$

A curious property of the anomalous contributions is the fact that at small K_F they are proportional to K_F, whereas the "normal" ones are proportional to K_F^3.

The expression for the complete four-point diagram $\Lambda^{(4)}$, as follows from (2.13), consists of (11.7) and an increment $\Lambda_\mu^{(4)}$, which in this approximation is equal to (see (2.14))

$$\Lambda_{\mu 0}^{(4)}(\mathbf{q}_1, -\mathbf{q}_1, \mathbf{q}_2, -\mathbf{q}_2) = \frac{1}{24}\frac{m^3}{\pi^2K_Fq_1q_2}\ln\left|\frac{2K_F+q_1}{2K_F-q_1}\right|\ln\left|\frac{2K_F+q_2}{2K_F-q_2}\right|. \quad (11.9)$$

A direct use of expressions (11.1), (11.2), (11.6), etc., corresponding to the ring diagrams, obviously conforms to an approximation of the self-consistent-field type, in which rescattering of electrons by screened ions, without exchange with the perturbed background, is taken into account. This approximation, which is valid in the case of high densities, is of limited accuracy at the typical densities in metals. Unfortunately, the electron gas has no small parameter at these densities, and it has therefore been impossible to develop so far a regular technique appropriate to the problem and with controllable accuracy.

However, in spite of the difficulties, progress has been made recently in the analysis of this problem, by using certain self-consistent schemes or by attempting to select and summarize entire classes of diagrams. All these efforts consist of investigations of the dielectric constant of a homogeneous gas, and lead to a polarization operator that can be represented in the static case in the form

$$\pi(\mathbf{q}) = \frac{\pi_0(\mathbf{q})}{1-(4\pi e^2/q^2)G(\mathbf{q})\pi_0(\mathbf{q})}. \quad (11.10)$$

Only the functions G(q), which play the role of the effective electron electron interaction, are different.

The first attempt to go outside the RPA framework was made by Hubbard[60], who attempted to summarize approximately the simplest class of exchange diagrams. As a result he arrived at an expression of the type (11.10) with

$$G_H(\mathbf{q}) = \frac{1}{2}\frac{q^2}{q^2+K_F^2}. \quad (11.11)$$

In this form, however, $\pi(\mathbf{q})$ does not satisfy the identity (4.9). Several modifications of (11.11) were subsequently proposed. The most frequently used form was that introduced by Geldart and Vosko[37]:

$$G_{HGV}(\mathbf{q}) = \frac{1}{2}\frac{q^2}{q^2+\xi K_F^2}, \quad (11.12)$$

where the parameter ξ was obtained precisely from the condition that (11.10) satisfy the identity (4.9). Inasmuch as we have already noted in Chap. 5, the compressibility κ is determined from the energy with sufficiently high accuracy, the values of $\pi(0)$, and at the same time also $\epsilon(q)$ at small q were determined in this case with perfectly reasonable accuracy. At metallic densities, the principal role in the compressibility is played by the exchange term (see, e.g.[4]) and

$$\xi = \frac{2}{1+(0.0155\pi/K_Fa_B)} \approx 2. \quad (11.13)$$

The next step was made in a recent group of studies by Geldart and Taylor[61-63], in which an attempt was made to select the most essential class of diagrams for the static polarization operator. The mutual cancellation of definite aggregates of diagrams, which is strongly pronounced in the Coulomb case, was traced during each stage. Particular attention was paid also to the need for satisfying the identity (4.9).

An entirely different approach, but one leading to close results for the same region of q, was developed at Argonne[64-66]. They made an approximate attempt to include, in a self-consistent manner, the corrections for the local field, with an aim at taking the correlations at short distances between the electrons into account, using a pair-correlation function for this purpose.

An approach based on the method of uncoupling the equations of motion for the Green's function was proposed by Toigo and Woodruff[67-69]. In principle, such a technique may turn out to be quite useful for this problem. A study of $\epsilon(\mathbf{q})$ is reported also in a number of papers (see[70-73]).

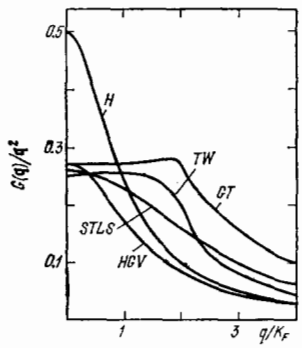

FIG. 10. Effective-interaction function G(q) in different theories: H–Hubbard, TW–Toigo-Woodruff, GT–Geldart-Taylor, STLS–Singwi-Tosi-Land-Sjolander, HGV–Hubbard-Geldart-Vosko.

We note that in the dynamic matrix, and when the static properties are described, we are interested actually in the behavior of the static polarization operator only at $q \lesssim 2K_F$. The abrupt decrease of $\pi_0(q)$ at $q > 2K_F$ makes the error in the determination of G(q) negligible in this region. At $q \lesssim 2K_F$, however, all the recent papers give a relatively similar behavior of G(q) (Fig. 10), which can be assumed to represent the true behavior in this region with reasonable accuracy.

It is possible also to improve accordingly the approximation for the irreducible many-point diagrams. To this end, we note that the total irreducible polarization operator is described by the following diagram:

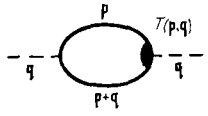

Analyzing the approximations that lead to (11.10), we can easily understand that they are actually equivalent to replacing the exact vertex by an approximate one that depends only on the momentum transfer (and letting $G(\mathbf{p}) \to G_0(\mathbf{p})$):

$$T(\mathbf{p}, \mathbf{q}) \approx T(\mathbf{q}) = \frac{1}{1-(4\pi e^2/q^2)\, G(\mathbf{q})\, \pi_0(\mathbf{q})}. \qquad (11.14)$$

Proceeding analogously for many-point diagrams, i.e., taking into account at each vertex the possibility of exchange and of correlation of the electron with the screening background, we obtain

$$\Gamma^{(n)}(\mathbf{q}_1, \ldots, \mathbf{q}_n) = \frac{\Lambda_0^{(n)}(\mathbf{q}_1, \ldots, \mathbf{q}_n)}{\tilde{\varepsilon}(\mathbf{q}_1) \ldots \tilde{\varepsilon}(\mathbf{q}_n)} \qquad (11.15)$$

($\Lambda_0^{(n)}$ is a ring n-point diagram); here

$$\tilde{\varepsilon}(\mathbf{q}) = \frac{\varepsilon(\mathbf{q})}{T(\mathbf{q})} = 1 + \frac{4\pi e^2}{q^2}(1 - G(\mathbf{q}))\, \pi_0(\mathbf{q}). \qquad (11.16)$$

We note, and this is quite important, that the approximations for all the irreducible many-point diagrams turn out to be reconciled in this case, in the sense that the hierarchy of the identities (4.6) is automatically satisfied, since we can show directly for ring diagrams, with the aid of the representation (8.9), that

$$\Lambda_0^{(n+1)}(\mathbf{q}_1, \ldots, \mathbf{q}_{n_0}) = -\frac{1}{n+1}\frac{d\Lambda^{(n)}(\mathbf{q}_1, \ldots, \mathbf{q}_n)}{d\mu}. \qquad (11.17)$$

12. MANY-PARTICLE PROBLEM WITH ALLOWANCE FOR NONLOCALITY OF THE ELECTRON-ION INTERACTION

So far, the entire analysis was carried out assuming locality of the vertex of the electron-ion interaction, corresponding to the substitution (2.3) in the initial Hamiltonian (2.1). From the fundamental point of view, the nonlocality of the potential introduces no new physical aspects into the problem, and all the qualitative results remain unchanged, but formal allowance for the nonlocality leads to certain complications in the scheme of the many-particle theory. The reason is that the problem is no longer factorized into separate ionic and electronic components, since the vertices of the electron-ion interaction, which now depend on the initial momentum, enter in the integrand (Fig. 11).

We shall consider specially only the question of the energy, bearing in mind the fact that the transition to the dynamical matrix and to other quantities remains the same as in the case of the local potential. If we forgo

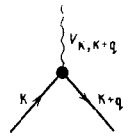

FIG. 11

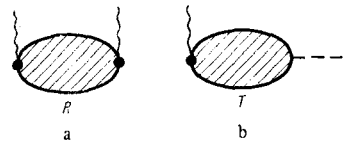

FIG. 12

(2.3), then the diagram (see Fig. 2) yields obviously for $E^{(1)}$ in place of (2.9)

$$E^{(1)} = \sum_{\mathbf{k}} V_{\mathbf{k},\mathbf{k}} n_{\mathbf{k}}. \qquad (12.1)$$

For the energy $E^{(2)}$ we can similarly use the same diagram representation as before (see Fig. 3). Now, however, characteristic blocks which are irreducible in the electron-electron interaction (Figs. 12a and 12b) appear and are no longer expressed in terms of the irreducible polarization block $\pi(\mathbf{q})$. Summing over all the polarization blocks that are strong on the electron-electron interaction line, we obtain (Fig. 12)

$$E^{(2)} = \frac{1}{2}\sum_{\mathbf{q}} \left| \frac{1}{N}\sum_{n} e^{i\mathbf{q}\mathbf{R}_n} \right|^2 \left\{ R(\mathbf{q}) - \frac{4\pi e^2}{q^2 \varepsilon(\mathbf{q})} |T(\mathbf{q})|^2 \right\}. \qquad (12.2)$$

In the local case we have $R(\mathbf{q}) = V_{-\mathbf{q}} T_{\mathbf{q}} = |V_{\mathbf{q}}|^2 \pi(\mathbf{q})$ and expression (12.2) reduces to the usual expression (2.15). The simplest approximation corresponding to the RPA approximation consists of neglecting (in the nonlocal case) the electron-electron interaction in $R(\mathbf{q})$ and $T(\mathbf{q})$:

$$R(\mathbf{q}) = \int \frac{d^3\mathbf{k}}{(2\pi)^3} \frac{n_{\mathbf{k}} - n_{\mathbf{k}+\mathbf{q}}}{\varepsilon_{\mathbf{k}} - \varepsilon_{\mathbf{k}+\mathbf{q}}} |V_{\mathbf{k},\mathbf{k}+\mathbf{q}}|^2, \qquad (12.3)$$

$$T(\mathbf{q}) = \int \frac{d^3k}{(2\pi)^3} \frac{n_{\mathbf{k}} - n_{\mathbf{k}+\mathbf{q}}}{\varepsilon_{\mathbf{k}} - \varepsilon_{\mathbf{k}+\mathbf{q}}} V_{\mathbf{k},\mathbf{k}+\mathbf{q}}.$$

Substituting everything in (12.2), we arrive at an expression for $E^{(2)}$ coinciding with the expression usually employed in practice in the case of a nonlocal potential [74].

It is of interest to separate in explicit form the screening of the nonlocal potential. In graphic form, the corresponding expression coincides with Fig. 4, when account is taken of the complication with the vertex (see Fig. 11). In analytic form this corresponds to

$$\tilde{V}_{\mathbf{k},\mathbf{k}+\mathbf{q}} = V_{\mathbf{k},\mathbf{k}+\mathbf{q}} + V_{sq}(\mathbf{q}), \qquad (12.4)$$

$$V_{sq}(\mathbf{q}) = -T(\mathbf{q})\frac{4\pi e^2}{q^2 \varepsilon(\mathbf{q})}. \qquad (12.5)$$

The screening potential $V_{sq}(\mathbf{q})$ is thus always local. If the initial potential is also local, then we arrive at the natural expression

$$\tilde{V}_{\mathbf{k},\mathbf{k}+\mathbf{q}} \to U_q/\varepsilon(\mathbf{q}), \qquad (12.6)$$

which was indeed used by us to separate the irreducible blocks (2.12). Now when the screening potential ($V_{sq}(\mathbf{q})$) is substituted in (12.2) instead of one of the $T(\mathbf{q})$, we can obtain another general representation of $E^{(2)}$. In the approximation (12.3), this representation corresponds to the following widely-used form:

$$E^{(2)} = \frac{1}{2}\sum_{\mathbf{q}} \left| \frac{1}{N}\sum_{n} e^{i\mathbf{q}\mathbf{R}_n} \right|^2 \int \frac{d^3\mathbf{k}}{(2\pi)^3} \frac{n_{\mathbf{k}} - n_{\mathbf{k}+\mathbf{q}}}{\varepsilon_{\mathbf{k}} - \varepsilon_{\mathbf{k}+\mathbf{q}}} V_{\mathbf{k},\mathbf{k}+\mathbf{q}} \tilde{V}_{\mathbf{k}+\mathbf{q},\mathbf{q}}. \qquad (12.7)$$

We consider now an arbitrary term $E^{(n)}$ with $n > 2$. This term is determined by a block with n external-field ends (see Fig. 1), where all the vertices again depend on the electron momenta before and after the scattering, and must therefore be included in the general integration of each diagram. It is interesting that in this case one can carry out a partial summation that leads to a replacement of each external-field line by a "thick" line,

which at this instant is equivalent to the substitution $V_{k,k+q} \to \tilde{V}_{k,k+q}$.

We present here in explicit form an expression (analogous to (12.7)) corresponding to allowance for only ring diagrams, i.e., without electron-electron interaction lines inside the ring (see the discussion in Chap. 11):

$$E^{(3)} = \frac{1}{3} \sum_{\mathbf{q}_1, \mathbf{q}_2, \mathbf{q}_3} \frac{1}{N^3} \sum_{n_1 n_2 n_3} \exp\left(i\mathbf{q}_1\mathbf{R}_{n_2} + i\mathbf{q}_2\mathbf{R}_{n_3} + i\mathbf{q}_3\mathbf{R}_{n_3}\right) Q^{(3)}(\mathbf{q}_1, \mathbf{q}_2, \mathbf{q}_3)\,\Delta(\mathbf{q}_1+\mathbf{q}_2+\mathbf{q}_3),$$

$$Q^{(3)}(\mathbf{q}_1, \mathbf{q}_2, \mathbf{q}_3) = \frac{2}{i}\int \frac{d^3\mathbf{p}\,d\omega}{(2\pi)^4} \tilde{V}_{\mathbf{p},\,\mathbf{p}+\mathbf{q}_1} \tilde{V}_{\mathbf{p}+\mathbf{q}_1,\,\mathbf{p}+\mathbf{q}_1+\mathbf{q}_2} \tilde{V}_{\mathbf{p}+\mathbf{q}_1+\mathbf{q}_2,\,\mathbf{p}} \times G^{(0)}(\mathbf{p}, \omega)\, G^{(0)}(\mathbf{p}+\mathbf{q}_1, \omega)\, G^{(0)}(\mathbf{p}+\mathbf{q}_1+\mathbf{q}_2, \omega), \qquad (12.8)$$

where the Green's function of the electron is defined in accordance with (8.1). We note that the integration with respect to ω is carried out in this expression in just as elementary a manner as before.

In the case of a local potential, the relation (12.6) holds true and we have

$$Q^{(3)}(\mathbf{q}_1, \mathbf{q}_2, \mathbf{q}_3) \to \frac{V(\mathbf{q}_1)}{\varepsilon(\mathbf{q}_1)} \frac{V(\mathbf{q}_2)}{\varepsilon(\mathbf{q}_2)} \frac{V(\mathbf{q}_3)}{\varepsilon(\mathbf{q}_3)} \Lambda_0^{(3)}(\mathbf{q}_1, \mathbf{q}_2, \mathbf{q}_3),$$

where $\Lambda^{(3)}$ is the three-point diagram obtained in Chap. 11. For arbitrary n, the expression for $E^{(n)}$ has an analogous structure.

From the form of the expressions and from an analysis of the general initial formulas we can deduce that all the general results remain fully in force in the case of a nonlocal potential. This pertains, in particular, to the ratio of the dynamic and static compressibilities, to the position and the character of the singularities in the phonon spectrum, to the unpaired character of the indirect inter-ion interaction, etc. (Allowance for the nonlocality does not change by itself the picture of the interaction between the ions in a metal, and consequently, is by no means an alternative for taking the many-particle forces into account, as is sometimes stated.)

A correct description of the qualitative picture, while analytically simple, makes the approximation corresponding to a local effective electron-ion interaction attractive whenever the physical aspect of the results is of primary importance.

13. ROLE OF ELECTRONS IN THE FORMATION OF THE EQUILIBRIUM LATTICE OF A METAL

The microscopic theory developed in the preceding chapter has made it possible to describe by means of a single scheme, using the same quantities, both the vibrational spectrum and the equilibrium structure of the metal.

In this chapter we wish to reveal certain general regularities that explain the role of the electrons in the formation of the static lattice in a real metal. We are interested in the character of formation of both the equilibrium density and the equilibrium crystallographic structure.

The first and simpler problem was already qualitatively considered in Chap. 7. For a quantitative illustration, Fig. 13 shows a plot of the total energy and of its individual contributions against the volume of the unit cell for Na.[41] We see that the role of the structurally-dependent terms $E^{(2)}$ and $E^{(3)}$ in Na is indeed very small. The equilibrium density is primarily the result of competition between the ion energy $E_i \sim \Omega_0^{-1/3}$ and the energy $E^{(1)} \sim \Omega_0^{-1}$. This remains qualitatively valid also for other nontransition metals, so that the zero model introduced above (see Chap. 7) accounts correctly for the main regularities in the formation of the equilibrium volume.

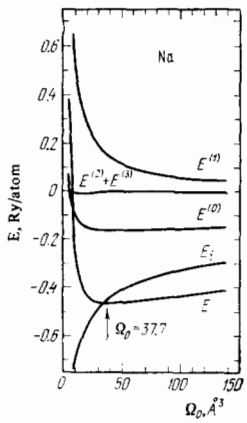

FIG. 13. Dependence of the total energy of Na and of its individual contributions on the volume Ω_0 of the unit cell.

If it is recognized that E_i depends relatively little on the structure, and that $E^{(1)}$ (as well as $E^{(0)}$) does not depend on it at all, then it becomes clear that the equilibrium density is determined to a considerable degree independently of the structure, i.e., by the concrete configuration of the ions.

We note also that the presence of a minimum on the $E(\Omega_0)$ curve indicates a locally stable metallic phase. To ascertain whether this phase is absolutely stable, it is necessary to compare in principle with other phases, for example, the atomic or molecular phase.

The question of explaining the realization of any particular structure is much more subtle, since in this case the large volume terms drop out from consideration and it is necessary to investigate small structure-dependent terms.

We now examine the problem of explaining the "anisotropy" of uniaxial metals, i.e., how the considered theory explains the different c/a ratios for metals. We note first that the competition takes place now between the ion energy E_i and the electron energy $E^{(2)} + E^{(3)} + \ldots$ The ion energy is lowest in this case for close-packed structures. As to the most important electronic contribution, $E^{(2)}$, it reveals, as first noted by Heine and Weaire[2], a tendency to form anisotropic structures. This can be easily understood. Only the values of the potential at the reciprocal-lattice sites contribute to the electron energy of the static lattice (see (2.15)). It is clear from this expression that if the anisotropy is increased, i.e., if some of the reciprocal-lattice sites are shifted to a region of smaller q, where V_q is stronger, we always gain in energy. However, very large distortions are certainly undesirable, owing to the sharp increase in the Ewald energy (the charges come closer together), so that the real situation at intermediate distortions depends on the scale of the potential.

These considerations are illustrated in Fig. 14 with Mg as an example[75]. We see that in Mg the electron energy has a tendency to anisotropy, but shifts c/a only slightly from the value corresponding to the minimum of the total energy (c/a = 1.636).

It appears that a similar situation obtains in metallic tin (β-Sn). Figure 15 shows the Madelung constant α_M

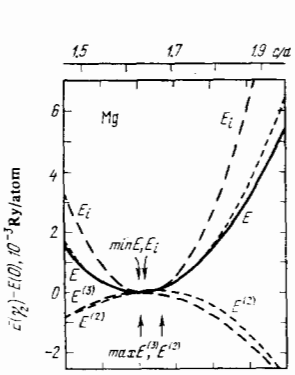

FIG. 14

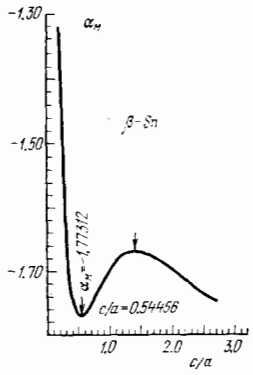

FIG. 15

FIG. 14. Dependence of the total energy of Mg and of its individual contribution on c/a.

FIG. 15. The Madelung constant for the ion energy in the structure of β-Sn as a function of c/a.

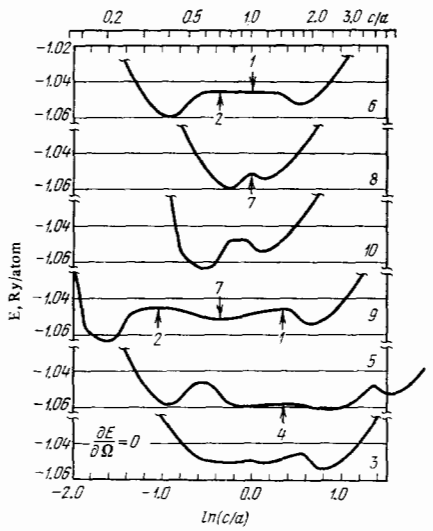

FIG. 16. Total energy of uniaxial lattices of metallic hydrogen as a function of c/a. Structures: 1–face-centered cubic (fcc), 2–body-centered cubic (bcc), 3–hexagonal close packed (hcp), 4–diamond, 5–white tin, 6–face-centerd tetragonal (fct), 7–primitive cubic (pc), 8–primitive tetragonal (pt), 9–trigonal (rhombohedral) (re), 10–primitive hexagonal.

for this structure as a function of c/a. It has a minimum at c/a = 0.545 close to the experimentally observed value (c/a = 0.553 at T = 0), so that the electronic contribution likewise shifts only insignificantly the minimum already present in the ion lattice. (We note that in the Ge lattice the value $c/a = \sqrt{2}$ corresponds to a maximum on this curve.) In principle, however, it is possible also to have a situation wherein the strong electron-ion interaction "wings" and leads to anisotropic structures.

By way of a clear-cut experiment we consider the metallic phase of hydrogen[30], where the electron-ion interaction constant is very large because of the absence of an ionic "core." Figure 16 shows the total energy as a function of c/a for a number of uniaxial structures (individual points correspond to cubic lattices). Anisotropy is observed everywhere, i.e., the electronic contribution prevails, the structures deviate from close-packed with "double-hump" curves and the distortion is strong in all cases. It is possible that a similar situation is realized in Zn and Cd, in which large deviations of c/a from the ideal value have been observed.

The foregoing examples and remarks explain the qualitative picture of the influence of electrons on the formation of an equilibrium structure of metals, the principal difference between which is precisely the presence of a subsystem of quasifree electrons.

14. ROLE OF ELECTRONS IN THE FORMATION OF THE PHONON SPECTRUM OF METALS

We now turn to the analysis of the general regularities in the influence of electrons on the formation of the phonon spectrum of metals.

It must be emphasized immediately that the study of such differential characteristics as the phonon spectrum offers a unique possibility of comparing the theoretical concepts with experiment, since we are dealing with the determination of the phonon spectrum in all of phase space. Accordingly, the results are sensitive to the behavior of both the electron-ion and electron-electron interactions for a continuous momentum interval, in contrast to the static quantities, which are determined by the corresponding values at discrete reciprocal-lattice points.

The role of the electrons is most clearly revealed if the vibration spectrum of the ion lattice of the metal is compared with the experimentally observed spectrum. Figure 17 shows curves for the Na lattice line and the experimental points[76]. The most significant changes occur, naturally, in the longitudinal branches, which turn from ionic plasma oscillations in the immobile background, when the electron "response" is taken into account, into acoustic oscillations. (For small momenta this question is discussed in detail in Chap. 4.) What is more unexpected is the fact that the ion lattice becomes attuned to the characteristic values of the frequencies, and that some transverse modes are in general very well described even in this approximation (a similar picture holds also for the shear moduli (see below)).

A much different situation is observed in metallic aluminum (Fig. 18; the experimental data are taken from the paper of Stedman et al.[77]). There the characteristic frequencies of the ion lattice at the end point of the band are already approximately double the corresponding

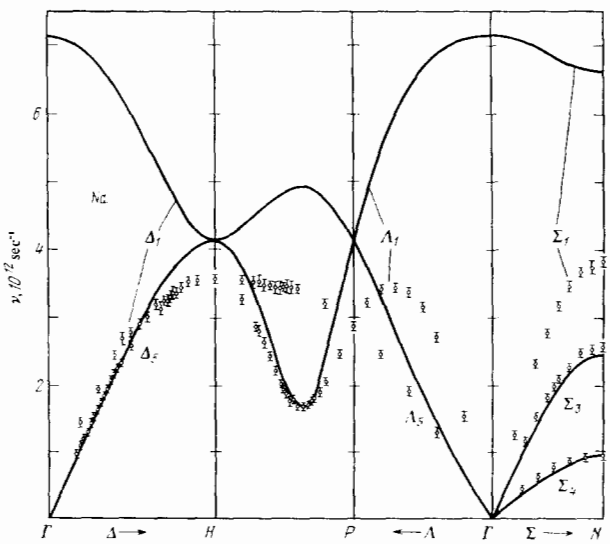

FIG. 17. Ion-lattice vibration frequencies and experimental frequencies of the phonons in Na.

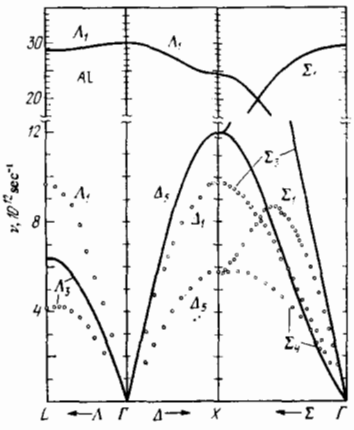

FIG. 18. Frequencies of ion-lattice vibrations and experimental frequencies of the phonons in Al.

experimental values. The compensation is even more appreciable for phonons in Pb. To illustrate the situation, Table I lists the values of $(\omega_i/\omega_0)^2$ and $(\omega_{exp}/\omega_0)^2$. Here ω_0 is the plasma ion frequency, which is a natural scaling characteristic of the spectrum, while ω_i^2 and ω_{exp}^2 were taken at the boundary of the Brillouin zone along [001].

TABLE I. Squares of frequencies in units of the plasma frequency

	Na	Al		Pb	
	L, $T(H_{15})$	$L(x_1)$	$T(x_5)$	$L(x_1)$	$T(x_5)$
$(\omega_i/\omega_0)^2$	0.333	0.678	0.161	0.678	0.161
$(\omega_{exp}/\omega_0)^2$	0.248	0.105	0.037	0.031	0.007

The table demonstrates the tremendous growth of the contributions from the electrons in the sequence Na, Al, Pb (see the analogous discussion in[9]). Thus, even an analysis of the experimental results without introduction of a concrete theoretical scheme allows us to conclude that the role of the electrons varies very strongly from metal to metal.

We shall now show that the microscopic theory makes it possible to explain in a perfectly natural manner the indicated regularity. We consider for simplicity the electron contribution in only the second approximation in the pseudopotential. We introduce for convenience the notation

$$\Psi(\mathbf{q}) = \frac{|V_{\mathbf{q}}|^2 \pi(q)\, q^2}{\varepsilon(\mathbf{q})} \frac{\Omega_0}{4\pi z^2 e^2}. \tag{14.1}$$

Then the electron contribution to the dynamical matrix of a monatomic metal takes, in accordance with (3.12), the form

$$D^{\alpha\beta}_{(2)}(\mathbf{q}) = -\omega_0^2 \Big[\sum_{\mathbf{K}} \frac{(\mathbf{q}+\mathbf{K})^\alpha (\mathbf{q}+\mathbf{K})^\beta}{|\mathbf{q}+\mathbf{K}|^2} \Psi(\mathbf{q}+\mathbf{K}) - \frac{\mathbf{K}^\alpha \mathbf{K}^\beta}{|\mathbf{K}|^2} \Psi(\mathbf{K}) \Big]. \tag{14.2}$$

For all three metals in all the symmetrical directions of $\mathbf{q}$ shown in Figs. 17 and 18, the dynamical matrix can be factored and the oscillations can be separated into purely transverse and purely longitudinal modes.

It is easily seen from an examination of the corresponding angles that the term with $\mathbf{K} = 0$ makes no contribution to the transverse oscillation modes, and we obtain

$$\omega_l^2 = \omega_{l1}^2 - \omega_0^2 \{ \Psi(\mathbf{q}) + \sum_{\mathbf{K}\neq 0} [\Psi(\mathbf{q}+\mathbf{K}) \cos^2(\widehat{\mathbf{e}_l, \mathbf{q}+\mathbf{K}}) - \Psi(\mathbf{K}) \cos^2(\widehat{\mathbf{e}_l, \mathbf{K}})] \}, \tag{14.3}$$

$$\omega_t^2 = \omega_{t1}^2 - \omega_0^2 \{ \sum_{\mathbf{K}\neq 0} [\Psi(\mathbf{q}+\mathbf{K}) \cos^2(\widehat{\mathbf{e}_t, \mathbf{q}+\mathbf{K}}) - \Psi(\mathbf{K}) \cos^2(\widehat{\mathbf{e}_t, \mathbf{K}})] \}, \tag{14.4}$$

Thus, the transverse modes of the oscillations are screened only with the aid of "Umklapp processes" and receive no contribution from the "continuous medium." (This circumstance is already discussed in connection with the problem of the shear moduli in Chap. 4). It is obvious from (14.3) and (14.4) that the character of the behavior of $\Psi(\mathbf{q})$ and the location of the reciprocal-lattice vectors for the given concrete metal become very important.

Figure 19 shows the function $\Psi(\mathbf{q})$ for Na, Al, and Pb, and indicates the locations of the lattice points; for the sake of uniformity, we used the calculations of Animalu[78] within the framework of the Abarenkov-Heine model. (For convenience, a section of the figure is shown enlarged.)

It is clear now that the decisive circumstance for Na is precisely the distribution of the reciprocal-lattice points, the closest of which is located much farther to the right than q_0, which is the first zero of V_q. This obviously corresponds to the fact that in monovalent Na the Fermi surface lies entirely in the first Brillouin zone, i.e., $2K_F < K_{min}$, and q_0 is usually even somewhat smaller than $2K_F$. As a result, the terms with $\mathbf{K} \neq 0$ in (14.3) and (14.4) play a very minor role, so that they transverse oscillation modes in Na are determined almost completely by the ionization lattice (especially at small $\mathbf{q}$). As to the longitudinal modes, the principal term for the electronic contribution is the one with $\mathbf{K} = 0$ in (14.3). It is easily seen that the electronic contribution to the longitudinal phonons is determined at the boundary of the band principally by the value of $\Psi(\mathbf{q})$ at $\mathbf{q}$ equal to half the distance to the corresponding site, and therefore it likewise screens the ion lattice weakly in Na. It is obvious here, in full accord with Fig. 17, that the values of the frequencies should be most strongly shifted for $\mathbf{q}$ in the direction [001].

The nearest reciprocal-lattice points in Al and Pb lie much closer than in Na, this being obviously due to the fact that Al and Pb are polyvalent metals. Therefore, first, an essential role is assumed by the terms of $\mathbf{K} \neq 0$, and, second, the term corresponding to the "continuous medium" on the boundary of the Brillouin zones is quite large. All this explains the appreciable enhancement of the role of the electrons, and it is clear from Fig. 19 that the behavior of $\Psi(\mathbf{q})$ and the disposition of the lattice sites indicate that the maximum electronic contribution is made precisely in Pb.

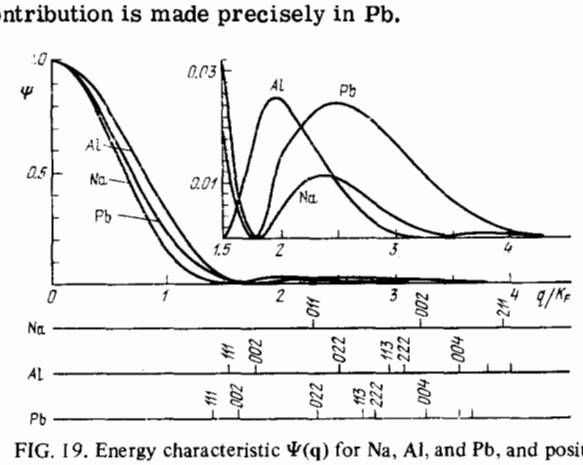

FIG. 19. Energy characteristic $\Psi(\mathbf{q})$ for Na, Al, and Pb, and positions of the corresponding reciprocal-lattice sites.

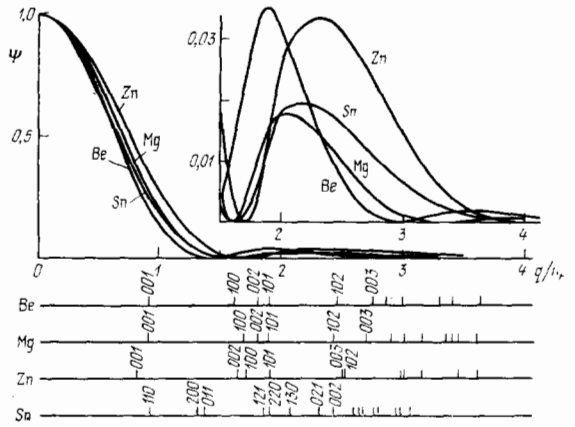

FIG. 20. Energy characteristic $\Psi(\mathbf{q})$ for Be, Mg, Zn, and Sn, and positions of the sites of the corresponding reciprocal lattices.

Even more interesting possibilities for the comparison of theory with experiment are provided by an analysis of diatomic metals in which there are optical frequencies. Let us consider the limiting optical frequencies at $\mathbf{q} = 0$, and designate them $\omega_c^2(0)$ and $\omega_a^2(0)$ in accordance with the oscillation polarizations (in uniaxial crystals, the two frequencies $\omega_a^2(0)$ are degenerate). Table II lists the data for these frequencies in Be, Mg, Zn, and β-Sn (using the same notation as in Table I). We see that for each element there is a low frequency, to which the electrons make a small contribution, and a high frequency, where this contribution is appreciable. To explain this result[15,6], we use expression (4.19), which we rewrite to conform with the notation in (14.1):

$$\omega_s^2(0) = \omega_{si}^2(0) - \omega_0^2 \sum_{\mathbf{K}\neq 0} \Psi(\mathbf{K}) \cos(\widehat{\mathbf{K}, \boldsymbol{\rho}}) \cos^2(\widehat{\mathbf{e}_s, \mathbf{K}}); \qquad (14.5)$$

here $\boldsymbol{\rho}$ is the basis vector of the second atom and $\mathbf{e}_s$ is the polarization of the oscillation mode.

With the aid of Fig. 20, which shows the function $\Psi(\mathbf{q})$ for the corresponding elements, we can explain the data listed in Table II. Indeed, the factor $\cos(\mathbf{e}_s, \mathbf{K})$ makes the roles of the individual reciprocal-lattice sites quite different for frequencies with different polarizations. In hexagonal metals, the "strongest" sites [001] contributes only to the screening of $\omega_c^2(0)$, and in tin the site [110], to the contrary, strongly screens just the frequency $\omega_a^2(0)$. All the other frequencies are weakly screened. In addition, it is clearly seen from Fig. 20 that the intensity of the screening due to the site [001] increases in the sequence Be, Mg, and Zn, in agreement with the data listed in Table II. Thus, the unique behavior of the optical frequencies is also naturally explained in the microscopic theory. We note incidentally that the foregoing considerations not only explain the variation of the electronic screening from metal to metal, but also show how a strongly anisotropic oscillation spectrum is reduced, only as a result of the location of the reciprocal-lattice sites, even if the interaction $V(|\mathbf{q}|)$ is isotropic.

We now examine the role of the electrons in the dynamic stabilization of the metal lattice. As already noted, the sum of all the forces acting on a given atom in the equilibrium position is always equal to zero in symmetrical lattices, and is equal to zero in other lattices, such as bismuth, under certain conditions. This means that a stationary point corresponds to a given configuration. This situation, however, can correspond not only to a minimum but also to a maximum or to a saddle point. The lattice is then dynamically unstable and imaginary oscillation frequencies appear. It is natural to distinguish between long-wave elastic instability, i.e., instability relative to a definite homogeneous deformation, and a short-wave instability, corresponding to phonons with finite momenta.

TABLE II. Squares of frequencies in units of the plasma frequency

	Be		Mg		Zn		β-Sn	
	(z)	(x, y)	(z)	(x, y)	(z)	(x, y)	(z)	(x, y)
$(\omega_i/\omega_0)^2$	0.890	0.055	0.906	0.047	0.953	0.024	0.001	0.499
$(\omega_{exp}/\omega_0)^2$	0.166	0.074	0.175	0.046	0.121	0.026	0.007	0.066

It was shown for the first time in[15,16], with β-Sn and Zn as examples, that the ion lattice of real metals can have dynamic instability. The corresponding results are given in Figs. 21 and 22. We see that the instability has a complicated character, and there are examples of both long-wave and short-wave instability. Thus, the ion lattices of Sn and Zn, while stable against variation of (c/a) (see Fig. 15), are unstable against more complicated deformations.

Indirect interaction by the electrons stabilizes the lattice, as is clear even from the very existence of these metals in the corresponding crystalline phases. As already noted in Chap. 4, the terms starting with $n \geq 3$ in the expansion of the energy assume an important role in the general case. The presently available quantitative analysis of β-Sn[15] and Zn[55] shows that when a potential of the Abarenkov-Heine type is used, the dynamic instability remains in both metals if only $D_{(2)}$ is taken into account. This raises the general question, whether the existence of unpaired inter-ion forces proper is of fundamental importance for the stability of such metals, or whether such a stability can be attained via paired forces only. This question is all the more interesting because as shown in Chap. 10, the terms of higher order in the potential also contain a paired part of the interaction. There is no rigorous answer to this question. A correct separation of the non-paired interaction together with a refinement of the electron-ion potential could explain the situation to a considerable degree, at least for concrete metals. It seems to us, however, that in metals such as metallic tin the multi-ion forces of the covalent type should certainly play an important role in the dynamic stabilization of the lattice.

We note that the electron contribution cannot only stabilize the lattice but, if the electron-ion potential is strong, "overscreen" the direct ion-ion interaction. Thus, for metallic hydrogen (at P = 0) all the cubic lat-

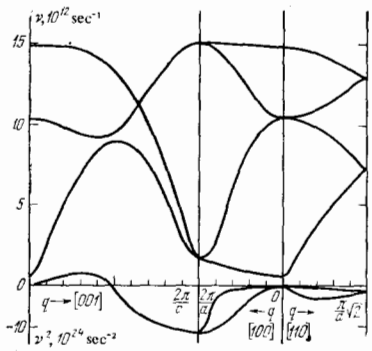

FIG. 21. Ion-lattice vibration frequencies for β-Sn.

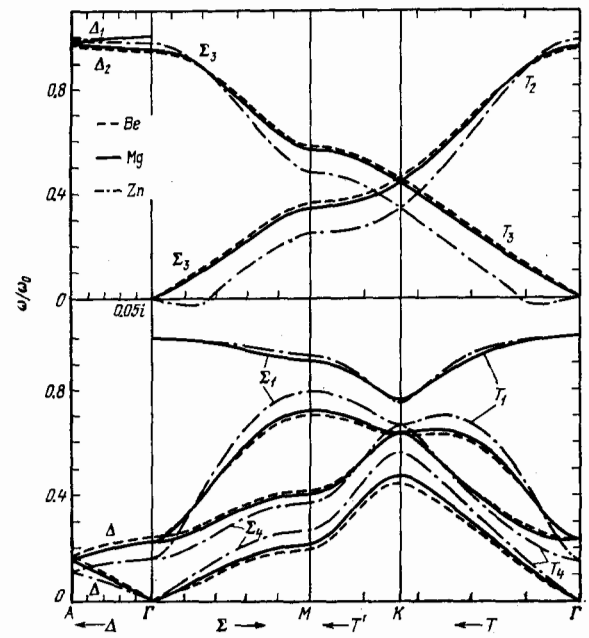

FIG. 22. Ion-lattice vibration frequencies for hexagonal metals (Be, Me, Zn).

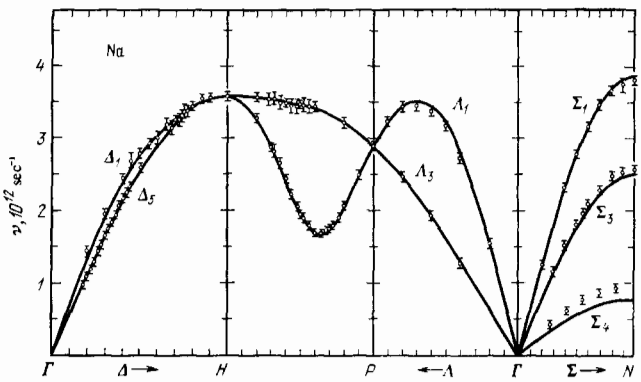

FIG. 23. Dispersion curves of phonons in Na.

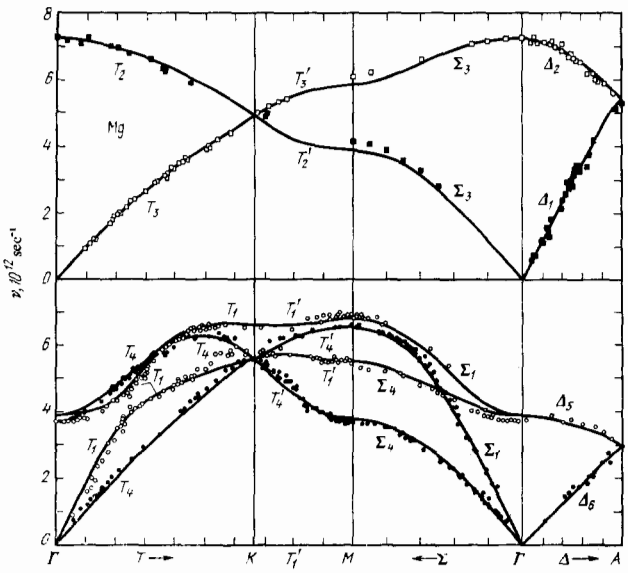

FIG. 24. Dispersion curves of phonons in Mg.

tices become unstable, although when only the ion-ion interaction is taken into account they are of course, stable[30]. Therefore, only strongly anisotropic structures are stable in this case. At high pressures, however, the role of the direct ion-ion interaction becomes predominant and accordingly the cubic lattices of metallic hydrogen are stable[79].

So far we have considered principally the qualitative picture of the formation of the phonon spectrum in a static metal lattice. However, the microscopic theory developed above makes it possible also to present a complete qualitative description of this entire aggregate of properties.

By way of illustration, let us examine certain results obtained for Mg[75], Na[28,41], and Al[28]. The choice of these metals is not accidental, being connected with the fact that a detailed analysis of their Fermi surfaces indicates that the nonlocality of the effective electron-ion interaction plays a minor role[80,81,82]. This makes the representation of a model pseudopotential in the simple local form reasonable (see[41,75]). The free parameters (two for Na and Al and three for Mg) are determined within the framework of the "inverse" problem with the aid of the corresponding number of experimental quantities, one of them being always determined from the equilibrium condition (6.2), and in the case of Mg one more is determined from the condition that the energy be a minimum relative to c/a (see[75]).

Figures 23—25 show the phonon dispersion curves calculated for Na, Mg, and Al with allowance for the terms of third order in the pseudopotential, and also the experimental data from[76,77,83]. We see that there is very good agreement between the theoretical and experimental results. What is particularly important is the fact that, by using the same pseudopotential, we can also present a quantitative description of the basic static characteristics of the metal. Table III lists, with magnesium as an example, the following data: the energy E, the pressure P, the bulk modulus B_{11}, the shear moduli B_{22}, B_{12}, B_{44}, and $B_{33} - [(B_{68})^2/B_{88}]$ connected with the usual c_{ik} (see[75]), and also the two limiting optical frequencies B_{88} and B_{99} at q = 0. In all cases, good quantitative agreement is observed between theory and experiment (a similar situation holds also for Na and Al[28]); this is far from trivial in matter, since the electrons play quite different roles in the different quantities. It is also quite interesting that, without varying the pseudopotential and by varying only the electron density it is possible to calculate, with sufficient accuracy, also the properties of the metal under pressure. For example, Fig. 26 shows the null isotherm P = P(Ω) for Mg in a wide range of pressures (Drickamer's experimental point[84]). The equation of state for Na was given above (see Fig. 5).

Figure 27 shows the Fourier component of the employed model potential, the points being the values of the pseudopotential obtained from an analysis of the Fermi surface of magnesium[80]. A comparison shows that the chosen pseudopotential should reproduce fairly well also the electronic spectrum near the Fermi surface. (We note, to be sure, that the question of the convergence in "pseudopotential" band calculations has not been sufficiently well investigated—see the discussion in[85]).

Returning to Table III, we can estimate the role of the individual contributions to different physical quantities,

TABLE III

Mg	E*	$B_1=P$	$B_{11}=B$	B_2	B_{22}	B_{12}	B_{44}	$B_{88}=\frac{\rho\Omega^2\omega_{11}^2}{4}$	$B_{99}=\frac{\rho\Omega^2\omega_0^2}{4}$	$B_{33}=B_{66}$	B_{68}	$B_{33}=-\frac{(B_{68})^2}{B_{88}}$
E_i	−2.1524	−6.82	−9.10	−0.0438	5.66	0.015	1.70	2.65	134.5	2.98	2.26	—
$E^{(0)}$	−0.2304	1.62	3.56	0	0	0	0	0	0	0	0	—
$E^{(1)}$	0.6705	6.38	12.76	0	0	0	0	0	0	0	0	—
$E^{(2)}$	−0.0906	−1.94	−5.79	0.0407	−1.19	−0.057	0.90	1.06	−97.7	0.19	−0.93	—
$E^{(3)}$	−0.0323	0.77	1.95	0.0031	−1.46	0.007	0.79	−0.93	−10.9	−1.04	0.55	—
E	−1.7705	0.00	3.38	0.0000	3.01	−0.035	1.81	2.78	26.0	2.13	0.78	1.91
Experiment	−1.7787 (±0.0060)	0.00	3.69	0.0000	3.01	−0.028	1.84	2.57	26.0	—	—	1.88

$$B_{11}=B=\frac{1}{9}(2c_{11}+2c_{12}+c_{33}+4c_{13}),\quad B_{22}=\frac{1}{9}(2c_{11}+2c_{12}+4c_{33}-8c_{13}),$$

$$B_{12}=\frac{1}{9}(2c_{13}+2c_{33}-2c_{11}-2c_{12}),\quad B_{33}-\frac{(B_{68})^2}{B_{88}}=\frac{1}{2}(c_{11}-c_{12}),\quad B_{44}=c_{44}.$$

*Energy in Ry/atom, elastic moduli in 10^{11} dyn/cm^2.

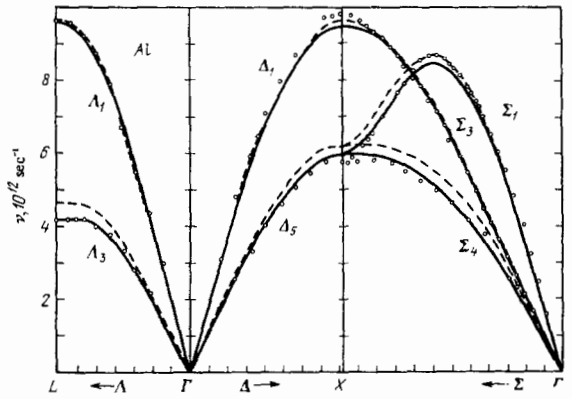

FIG. 25. Dispersion curves of phonons in Al (dashed curve—without D_3).

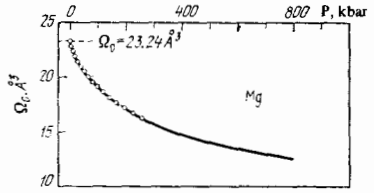

FIG. 26. Equation of state for Mg.

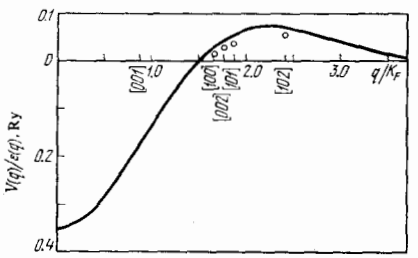

FIG. 27. Fourier component of the pseudopotential in Mg.

and particularly the contributions of third order in the pseudopotential. We see that in a number of cases they are quite appreciable, and increase from the energy to the elastic moduli. A direct estimate of these values for other metals, for example β-Sn[28,86] shows that they can determine in decisive manner, for example, the characteristic frequencies of the phonon-spectrum oscillations. A more detailed quantitative discussion of this question is contained in the review[28].

In conclusion, it should be specially noted that for certain metals the quantitative agreement between theory and experiment, if the same simple scheme is used to describe the electron-ion interaction, may be not so convincing as for Na, Mg, and Al. This, however, is of no fundamental significance (for example, for a given ion the interaction with the electron may be essentially nonlocal). What is important is that the macroscopic theory as developed to date, in which exact account is taken of the interaction in a metal, undoubtedly provides a reasonable quantitative description of the entire aggregate of the properties of the metal as a whole.

[1)] A more detailed analysis of this problem is contained in an article by the authors, published in the collection "Lattice Dynamics," edited by A. A. Maradudin and G. K. Harton, Amsterdam, North Holland, 1974.

[1] W. A. Harrison, Pseudopotentials in the Theory of Metals, Benjamin, 1966.
[2] V. Heine and D. Weaire, Sol. State Phys. **24**, 249 (1970).
[3] M. L. Cohen and V. Heine, ibid., p. 37.
[4] D. Pines and P. Nozieres, The Theory of Quantum Liquids, N.Y., Benjamin, 1966.
[5] M. Born and K. Huang, Dynamical Theory of Crystal Lattices, Oxford, U. Press, 1954.
[6] A. A. Maradudin et al., Theory of Lattice Dynamics in the Harmonic Approximation, Academic, 1971.
[7] W. Cochran, Inelastic Scattering of Neutrons, v. **1**, Vienna, IAEA, 1965, p. 3.
[8] T. Toya, J. Res. Inst. Catal. Hokkaido Univ. 6, 161, 183 (1958).
[9] S. H. Vosco, R. Taylor and G. H. Keech, Canad. J. Phys. **43**, 1187 (1965).
[10] L. J. Sham, Phys. Rev. **188**, 1431 (1969).
[11] R. M. Pick, M. H. Cohen and R. M. Martin, ibid. **B1**, 910 (1970).
[12] L. J. Sham, Proc. Roy. Soc. **A283**, 33 (1965).
[13] J. V. Koppel and A. A. Maradudin, Phys. Lett. **A24**, 224 (1967).
[14] J. V. Koppel, Ph. D. Thesis (San Diego, 1968).
[15] E. G. Brovman and Yu. Kagan, Zh. Eksp. Teor. Fiz. **52**, 557 (1967) [Sov. Phys.-JETP **25**, 365 (1967)].
[16] Yu. Kagan and E. G. Brovman, Neutron Inelastic Scattering, v. 1, Vienna, IAEA, 1968, p. 3.
[17] E. G. Brovman and Yu. Kagan, Zh. Eksp. Teor. Fiz. **57**, 1329 (1969) [Sov. Phys.-JETP **30**, 721 (1970)].
[18] G. V. Chester, Adv. Phys. **10**, 357 (1961).
[19] L. D. Landau, Zh. Eksp. Teor. Fiz. **30**, 1058 (1956) [Sov. Phys.-JETP **3**, 920 (1956)].
[20] A. B. Migdal, ibid. **34**, 1438 (1958) [**7**, 996 (1958)].
[21] S. V. Tyablikov, ibid. **34**, 1254 (1958) [**7**, 867 (1958)].
[22] S. K. Joshi and A. K. Rajagopal, Sol. State Phys. **22**, 159 (1968).
[23] A. A. Abrikosov, L. P. Gor'kov, and I. E. Dzyaloshinskiĭ, Metody kvantovoi teorii polya v statisticheskoi fizike (Quantum Field Theoretical Methods in Statistical Physics), Fizmatgiz, 1962 [Pergamon, 1965].
[24] G. M. Éliashberg, Zh. Eksp. Teor. Fiz. 38, 966 (1960) [Sov. Phys.-JETP **11**, 696 (1960)].
[25] J. E. Schrieffer, Theory of Superconductivity, N.Y., Benjamin, 1964.
[26] C. E. Monfort and C. A. Swenson, J. Phys. Chem. Sol. **26**, 291 (1965).
[27] E. G. Brovman and A. Holas, Zh. Eksp. Teor. Fiz. **66**, 1877 (1974) [Sov. Phys.-JETP **39**, No. 5 (1974)].
[28] E. G. Brovman and Yu. Kagan, in: Lattice Dynamics, Ed. A. A. Maradudin and G. K. Horton, Amsterdam, North-Holland, 1974.

[29] W. Kohn and J. M. Luttinger, Phys. Rev. **118**, 41 (1960).
[30] E. G. Brovman, Yu. Kagan and A. Holas, Zh. Eksp. Teor. Fiz. **61**, 2429 (1971) [Sov. Phys.-JETP **34**, 1300 (1972)].
[31] C. Baym, Ann. Phys. (N.Y.) **14**, 1 (1961).
[32] C. J. Pethick, Phys. Rev. **B2**, 1789 (1970).
[33] J. M. Luttinger and J. C. Ward, ibid. **118**, 1417 (1960).
[34] J. Bardeen and D. Pines, ibid. **99**, 1140 (1955).
[35] D. Bohm and T. Staver, ibid. **84**, 836 (1950).
[36] E. G. Brovman, Yu. Kagan, and A. Kholas, Zh. Eksp. Teor. Fiz. **57**, 1635 (1969) [Sov. Phys.-JETP **30**, 883 (1970)].
[37] J. W. Geldart and S. H. Vosco, Canad. J. Phys. **44**, 2137 (1966).
[38] A. D. B. Woods, B. N. Brockhouse, R. H. March, A. T. Stewart and R. Bowers, Phys. Rev. **128**, 1112 (1962).
[39] R. A. Cowley, A. D. B. Woods and G. Dolling, ibid. **150**, 487 (1966).
[40] E. G. Brovman, Yu. Kagan, and A. Kholas, ZhETF Pis. Red. **10**, 45 (1969) [JETP Lett. **10**, 30 (1969)].
[41] E. G. Brovman, Yu. Kagan, and A. Kholas, Fiz. Tverd. Tela **12**, 1001 (1970) [Sov. Phys.-Solid State **12**, 786 (1970)].
[42] N. Bernardes and C. A. Swenson, in: Solids under Pressure, Ed. W. Paul, N.Y., Warshauer, 1963.
[43] R. I. Beecroft and C. A. Swenson, J. Phys. Chem. Sol. **18**, 329 (1961).
[44] E. G. Brovman and Yu. Kagan, Zh. Eksp. Teor. Fiz. **63**, 1937 (1972) [Sov. Phys.-JETP **36**, 1025 (1973)].
[45] L. Landau, Nucl. Phys. **13**, 181 (1959).
[46] A. B. Migdal, Zh. Eksp. Teor. Fiz. **32**, 399 (1957) [Sov. Phys.-JETP **5**, 333 (1957)].
[47] J. Lindhard, J. Kgl. Dansk. Mat. Phys. Madd. **28**, 8 (1954).
[48] W. Kohn, Phys. Rev. Lett. **2**, 393 (1959).
[49] B. N. Brockhouse, K. R. Rao and A. D. B. Woods, ibid. **7**, 93 (1961).
[50] B. N. Brockhouse, T. Arase, C. Caglioti, K. R. Rao, and A. D. B. Woods, Phys. Rev. **128**, 1099 (1962).
[51] R. Stedman, L. Almqvist, and G. Nilsson, ibid. **162**, 545 (1967).
[52] A. M. Afanas'ev and Yu. Kagan, Zh. Eksp. Teor. Fiz. **43**, 1456 (1962) [Sov. Phys.-JETP **16**, 1030 (1963)].
[53] A. Ya. Blank and É. A. Kaner, ibid. **50**, 1013 (1966) [**23**, 673 (1966)].
[54] J. W. Weymouth and R. Stedman, Phys. Rev. **B2**, 4743 (1970).
[55] E. G. Brovman, Yu. Kagan, and A. Holas, in[16], p. 165.
[56] L. Almqvist and R. Stedman, J. Phys. **F1**, 785 (1971).
[57] A. P. Roy, B. A. Dasannacharya, C. L. Thaper, and P. K. Iyengar, Phys. Rev. Lett. **20**, 906 (1973).
[58] A. R. Williams and D. Weaire, J. Phys. **C3**, 386 (1970).
[59] P. Lloyd and C. A. Sholl, J. Phys. **C1**, 1620 (1968).
[60] J. Hubbard, Proc. Roy. Soc. **A243**, 336 (1957).
[61] J. W. Geldart and R. Taylor, Canad. J. Phys. **48**, 155 (1970).
[62] J. W. Geldart and R. Taylor, ibid., p. 167.
[63] J. W. Geldart and R. Taylor, Sol. State Comm. **9**, 7 (1971).
[64] K. S. Singwi, M. P. Tosi, R. H. Land, A. Sjolander, Phys. Rev. **176**, 589 (1968).
[65] K. S. Singwi, A. Sjolander, M. P. Tosi, and R. H. Land, ibid. **B1**, 1044 (1970).
[66] P. Vashista and K. S. Singwi, ibid. **B6**, 875 (1972).
[67] F. Toigo and T. O. Woodruff, ibid. **B2**, 3958 (1970).
[68] F. Toigo and T. O. Woodruff, ibid. **B4**, 4312 (1971).
[69] F. Toigo and T. O. Woodruff, ibid., p. 371.
[70] L. Kleinman, ibid. **160**, 585 (1967).
[71] L. Kleinman, ibid. **173**, 383 (1968).
[72] D. C. Langreth, ibid. **181**, 753 (1969).
[73] R. W. Shaw, J. Phys. **C3**, 1140 (1970).
[74] A. O. E. Animalu, Phil. Mag. **11**, 379 (1965).
[75] E. G. Brovman, Yu. Kagan, and A. Kholas, Zh. Eksp. Teor. Fiz. **61**, 737 (1971) [Sov. Phys.-JETP **34**, 394 (1972)].
[76] A. D. B. Woods, B. N. Brockhouse, R. H. March, A. T. Stewart, and R. Bowers, Phys. Rev. **128**, 1112 (1962).
[77] R. Stedman and G. Nilson, ibid. **145**, 492 (1966).
[78] A. O. E. Animalu, Proc. Roy. Soc. **A294**, 376 (1966).
[79] E. G. Brovman, Yu. Kagan, and A. Kholas, Zh. Eksp. Teor. Fiz. **62**, 1492 (1972) [Sov. Phys.-JETP **35**, 783 (1972)].
[80] J. C. Kimball, R. W. Stark, and F. M. Mueller, Phys. Rev. **162**, 600 (1967).
[81] M. J. G. Lee, Proc. Roy. Soc. **A295**, 440 (1966).
[82] N. W. Ashcroft, Phil. Mag. **8**, 2055 (1963).
[83] A. Pindor and R. Pynn, J. Phys. **C2**, 1037 (1969).
[84] G. Drickamer, Sol. State Phys. **17**, 1 (1965).
[85] J. P. Van Dyke, Phys. Rev. **B7**, 2358 (1973).
[86] E. G. Brovman and G. Solt, Sol. State Comm. **8**, 903 (1970).

Translated by J. G. Adashko